Pressure Transient Behaviour of Horizontal Wells in a Bounded Reservoir with Gas Cap and Aquifer

by

Tsani Sabila

17020

Dissertation submitted in partial fulfillment of

the requirements for the

Bachelor of Engineering (Hons)

(Petroleum)

MAY 2015

Universiti Teknologi PETRONAS

Bandar Seri Iskandar

31750 Tronoh

Perak Darul Ridzuan

CERTIFICATION OF APPROVAL

Pressure Transient Behaviour of Horizontal Wells in a Bounded Reservoir with Gas Cap and Aquifer

by

Tsani Sabila
17020

A project dissertation submitted to the
Petroleum Engineering Programme
Universiti Teknologi PETRONAS
in partial fulfillment of the requirement for the
BACHELOR OF ENGINEERING (Hons)
(PETROLEUM)

Approved by,	Approved by,
_____	_____
(Ms. Azeb Demisi Habte)	(Dr. Mohammed Abdalla Ayoub)

UNIVERSITI TEKNOLOGI PETRONAS

TRONOH, PERAK

May 2015

CERTIFICATION OF ORIGINALITY

This is to certify that I am responsible for the work submitted in this project, that the original work is my own except as specified in the references and acknowledgements, and that the original work contained herein have not been undertaken or done by unspecified sources or persons.

_____

TSANI SABILA

ABSTRACT

Increased productivity can be seen as a result of horizontal well applications in some certain reservoir conditions. Consequently, there exist the need to monitor the performance of the horizontal wells and characterising the reservoir surrounding it. The literature provided limited study on pressure transient behaviour of horizontal wells in a reservoir with vertical constant pressure boundaries and even lesser investigating completely bounded reservoir (in all x, y, z) directions. An analytical solution is thus presented for the pressure transient response of horizontal wells in an anisotropic, rectangular, homogeneous reservoir, bounded by gas cap and aquifer and laterally, by no-flow boundaries. Solutions were formulated using Green's and source function method in combination with Newman product method. Type curves analysis and detailed discussion of each flow regimes exhibited are thoroughly investigated. Different dimensions of rectangular-shaped reservoirs and the effects of varying distance of the horizontal well to outer boundaries are included in this study. It could be observed that the pressure behaviour and flow regimes exhibited depend on the type of outer boundaries, distance of the well to the nearest boundary and length of horizontal well itself. Common flow regimes usually associated with horizontal wells were masked by the constant pressure behaviour.

ACKNOWLEDGEMENTS

The author would like to express the deepest gratitude and appreciation to the following respective people for their support, patience and guidance.

- **FYP Supervisor, Ms. Azeb Demisi Habte** for her continuous support, time, persistent guidance and assistance throughout the progress of this research. Her never ending dedication and coaching in various aspects of this project had played a significant, vital role in ensuring the success of this research. With her dedicated assistance, the author was able to solve all the challenges encountered during the course of this project.

- **Lecturer, AP. Dr. Muhannad Talib Shuker** for his effective teaching during Advanced Well Test Analysis course. His technical expertise in well testing had greatly strengthened the author's fundamentals. As Dr. Muhannad was also the author's internal examiner; his feedback, advices and encouragement were much appreciated.

- **FYP Coordinators, Dr. Asif and Mr. Titus** for their continuous support and understanding. The author wishes to thank especially to Dr. Asif and respective examiners for all their kind understanding in accommodating for the author's unforeseen illness at the end of the FYP course (FYP II).

The author would also like to extend a token of appreciation to family and friends for their unwavering love, support and assistance throughout this project.

TABLE OF CONTENTS

LIST OF FIGURES

LIST OF TABLES

LIST OF EQUATIONS

CHAPTER 1: INTRODUCTION

1.1. BACKGROUND

The strategic practicalities and profitability of horizontal wells in certain reservoir situations have been widely-recognized and well-established in the oil and gas sector. Improved well productivity, increased well deliverability, reduction of the effects of damaged zones and higher oil recovery due to better sweep efficiency are all among direct results of using horizontal wells.

Due to its advantageous nature, over the past two decades, there has been rapid surge in the implementation of horizontal wells technology especially in situations where the conventional vertical method has either produced lesser amount than desired rate or ultimately failed. As a consequence of this, there also exist the need to develop analytical models that can evaluate the performance of these horizontal wells. An analytical model is used here because the analytical solution is able to give "meaning" especially when the variables are changed.

Transient pressure analysis techniques have emerged as an auspicious method for the assessment of horizontal well productivity and performance as well as reservoir characterisation. The majority of previous researchers used the technique of Green's source function that was developed by Gringarten and Ramey [1] to analyse horizontal wells in an anisotropic homogeneous system as analogous to vertical fractures.

A horizontal well has different flow geometry (3D) comparatively to that of a vertical well (1D symmetrical radial flow). Horizontal well's performance can be strongly influenced by the partial penetration and anisotropy of horizontal to vertical permeability. Instead of seeing the radial flow symmetry that is normally present in a vertical well test, several flow regimes may occur in horizontal well tests. When dealing with vertical wells, one may usually handle with variables such as average permeability, net vertical thickness, and skin. However, in horizontal well testing, more parameters are needed. Not only is the vertical thickness important, but horizontal dimensions of the reservoir, relative to horizontal wellbore, need to be known. Furthermore, other factors such as,

effective well length and vertical permeability can influence the transient pressure behaviour in a horizontal well test. The effect of wellbore storage is also more prominent in horizontal well testing as opposed to vertical well testing.

The literature provided limited study for an analytical solution pertaining horizontal wells in a reservoir bounded by vertical constant pressure boundaries apart from the research conducted by Lu [2] and Stewart and Du [3]. Yet, both research studies still did not consider completely bounded reservoir geometry in lateral directions (they considered laterally infinite boundaries). Even fewer were investigating the reservoir bounded in all 3 directions (x, y, z) with the exceptions of three analytical works [4] - [6], all of which focused on vertical no-flow boundaries.

Hence, the purpose of this study is to develop/formulate equations using the principles of Green's and source functions merged with Newman's [7] product method based on the results of Gringarten and Ramey's analysis [1] and combining with the dimensionless variables defined in Al Rbeawi and Tiab's work [5] to investigate the effects of both gas cap and aquifer and lateral no-flow boundaries on the transient pressure behaviour of horizontal wells in a homogeneous, anisotropic reservoir. Relevant type curves will be generated based on dimensionless pressure and pressure derivative for varying horizontal well parameters. Application of this work includes, but not limited to, characterising and managing horizontal wells in an oil rim.

1.2. PROBLEM STATEMENT

Recalling the numerous advantageous applications of horizontal wells as Goode and Thambynayagam elaborately explained in their study [8], hence, the subsequent need to monitor horizontal wells' performance and to characterise the reservoir surrounding it also becomes an important matter for project viability and economics.

Majority of the early researchers previously have concentrated on developing solutions for horizontal wells in an infinite-acting, anisotropic and homogeneous reservoir [2] - [5]. To the author's knowledge, the literature has provided limited investigation so far into providing analytical solution for reservoir geometry possessing vertical constant pressure boundaries with lateral no-flow boundaries (bounded in all 3 directions). Some may have taken into account only the vertical constant pressure boundaries in their reservoir geometry [2], [3] but still considered infinite lateral boundaries. Consequently, the aim of this work is to analyse the pressure transient behaviour of horizontal wells situated in a homogeneous, anisotropic reservoir bounded by a gas cap and aquifer with lateral no-flow boundaries.

1.3. OBJECTIVES AND SCOPE OF STUDY

1.3.1. OBJECTIVES

Primarily, the purpose of this work is to investigate the pressure transient behaviour of horizontal wells in anisotropic rectangular-shaped reservoir bounded vertically by gas cap and aquifer and, laterally by no-flow boundaries.

Particularly, this study aims to:

i. Analyse pressure transient behaviour of horizontal wells in the reservoir with the boundary conditions as mentioned above in order to obtain essential parameters for reservoir characterisation, evaluation and management
ii. Develop / generate relevant type curves for transient pressure interpretation of horizontal wells for varying horizontal well parameters with reservoir conditions as mentioned previously.

1.3.2. SCOPE OF STUDY

In this study, focus will be directed in analysing and interpreting pressure behaviour of horizontal wells in a homogeneous, rectangular-shaped reservoir bounded by vertical constant pressure boundaries and also, bounded by two no-flow boundaries laterally. The diffusivity equation to be solved is for 3D, anisotropic medium with cartesian coordinates. The assumption of slightly compressible fluid with constant compressibility and viscosity is applied throughout the medium. In addition, effects of gravity are negligible. The directions of permeability are indicated with k_x, k_y and k_z respectively. Negligible wellbore storage will be accounted here for simplification. Future studies will include effects of wellbore storage in the equation. Type curves will be constructed on the basis of analytical techniques obtained from previous studies' results using Green's/source function method [1] in combination with Newman product method for both short and long horizontal wells taking into consideration the effects of the outer vertical constant pressure boundaries and horizontal no-flow boundaries at the sides. The distance to the respective external boundaries in two directions and length of producing horizontal section is included. All flow regimes exhibited is thoroughly investigated.

CHAPTER 2: LITERATURE REVIEW AND THEORY

The beneficial applications of horizontal well technology have led to positive production increments in various reservoir situations. The key advantage of using horizontal wells is that production rate is increased due to more of the wellbore length being exposed to pay zone (larger surface/contact area). This has led the horizontal well technology being implemented for production enhancement and ultimate oil and gas recovery, particularly in formations with low-permeability.

Goode and Thambynayagam published a compilation of comprehensive case studies [8] proving several benefits of horizontal wells including one prominent case study located in the Adriatic Sea of the Italian area where the horizontal well productivity was 20 times greater than adjacent vertical and deviated wells. Among the reported case studies, Giger [9] also proved that the occurrence of water and gas influx can be deterred in multiphase flow. In addition, he also calculated higher sweep efficiency. Spivak [10] confirmed this fact and further described reduced water and gas coning which was also a resolved serious problem reported previously by Striegler [11]. Moreover, Chaudhry [12] also clarified that with the use of horizontal wells, the drainage area is increased whereas in high-permeability reservoirs; the turbulence in the near wellbore region is reduced and well deliverability is improved.

Al Rbeawi and Tiab [5] have also compiled other beneficial applications of horizontal wells including, but not limited to, unconventionals, applications in low-permeability reservoirs, in effectively intersecting and draining naturally-fractured reservoirs, in decreasing production wells in both low and high permeability gas reservoirs, in enhancing the contact between well and reservoir in tertiary recovery and lastly, to reduce the expenses of drilling and quantity of production facilities in environmentally sensitive places such as offshore fields.

Technically, the following are some of the main factors which contribute to incremental production as a result of horizontal wells technology application as published by SPE International [13].

1. Reduced drawdown for a specified production rate causes a decrease in water and gas coning. As a consequence, remedial work also decreased.
2. Longer wellbore length being exposed to pay zone increases the production rate
3. Around vicinity of the wellbore, pressure drop is reduced
4. Lesser sand production as a result of both items (2) and (3)
5. Enlargement of drainage pattern with more effectivity which then follows an increase in the recovery of overall reserves

The need and advantages of horizontal wells have clearly been observed as above. Hence, the subsequent need to monitor their performance and to characterise the reservoir surrounding it also becomes an important matter for project feasibility and economics. Over time, well testing has become a favourable method in accomplishing the above mentioned tasks.

Although many analytical models have been proposed for horizontal well test analysis; there still exist several limitations and uncertainties about the pressure behaviour governing the wellbore and outer boundaries. This is due to the complex variety of geometrical configurations and horizontal well completion techniques which leads to a deviation of pressure behaviour from the norms. In their book, Lee, Rollins and Spivey [14] explained the reasons for more complexity in the interpretation of pressure transient in horizontal wells as compared to vertical wells. Firstly, the major key challenge is that the flow geometry in horizontal wells is 3D as opposed to the radial symmetry present in a vertical well.

In addition, Chaudhry [12] further described that usually, we assume the wells to be situated ideally horizontal and parallel to the top and bottom outer boundaries of reservoir. In reality, wells are rarely perfectly horizontal. Secondly, negative skin factors makes calculations difficult. Thirdly, obtaining the production length of a long horizontal well proves to be a challenge as well. Furthermore, Al Rbeawi and Tiab [5] explained that diverse trends of the pressure derivative can occur subject to geometrical configuration of the overall system, zonal damage and the formation's own petrophysical properties

One of the foremost works were credited to Clonts and Ramey [15] in which they proposed the usage of line source approximation solution based on the analogy of partially penetrating vertical fracture to solve for horizontal well testing analysis.

Thereafter, Gringarten and Ramey [1] published a more comprehensive work using Green's and source functions in combination with other methods such as Lord Kelvin's [16] point source solution and Newman's product method mentioned earlier [7] to solve unsteady-flow anisotropic problems analytically. They combined several of these solutions mentioned as above due to realising that, for a given system, it's often difficult to obtain the Green's function. However, with the combination of product method proposed by Newman in heat conduction problems; it is possible to obtain a solution in which he proved that the product of three one dimensional heat conduction problems is equal to the solution of a three-dimensional problem. Similarly, this concept can also be applied to solving pressure distribution in a reservoir system. Gringarten and Ramey's [1] work provided a medium to solve diffusivity equation with various initial or boundary value conditions. Consequently, many successive researchers then extended their work to solve solutions for horizontal wells based on their theory to be applied in several other reservoir conditions.

Subsequently, Daviau et al [4] further extended their work to develop equations to solve for pressure transient behaviour in horizontal wells for several other possible reservoir geometries. All of their equations are based on Gringarten and Ramey's work [1].

Among the models developed in Daviau's study [4] included isotropic infinite-acting reservoir and two anisotropic reservoir models both bounded by vertical no-flow boundaries; each possessing varying lateral boundaries. Moreover, for horizontal wells in the anisotropic system, they formulated the equations for two homogeneous models; both models exhibit no flow vertical boundaries and varying lateral boundaries; (1) first model with impermeable lateral boundaries (2) while the second model with lateral constant pressure boundaries. The log-log and semi log analysis were also provided. Double-porosity system analysis using Laplace Transform was also presented. Their work, apart from Al Rbeawi and Tiab [5] and Xiadong [6] were among the only ones to investigate the effects of boundaries in all three directions (x, y, z).

On the contrary, Kuchuk, Goode, Wilkinson and Thambynayagam later in their work[17] used the same basis of analytical solutions combined with Fourier transforms to investigate anisotropic, homogeneous model exhibiting mixed vertical boundaries but laterally infinite boundaries. They solved for two models (1) control model bounded by no flow-boundaries at top and bottom and (2) second model bounded by mixed vertical boundaries (a model possessing one no-flow boundary and one constant-pressure boundary represented by a gas cap). Flow regimes that were exhibited included elliptic-cylindrical flow in early-time radial flow and linear flow in intermediate-time. Solutions using Laplace transform are used to include wellbore storage and skin effects in their analysis.

Stewart and Du [2] then published a comprehensive work regarding the effects of lateral boundaries on pressure transient behaviour of horizontal wells in an anisotropic, homogeneous system. They explored and provided a wide spectrum of analysis regarding the effects of various lateral boundaries geometries; among them included starting from laterally infinite reservoir to single boundary, parallel boundaries, intersecting no-flow boundaries in all three vertically bounded situations (formation top and bottom no flow, gas cap/aquifer, or mixed boundaries). However, their work did not consider the reservoir being bounded in all 3 directions (x, y, z). They always considered one of the lateral boundaries to be infinite, most of the time in the x-direction.

Al Rbeawi & Tiab [5] stated that most of these early theories were mainly based in assuming the system to be analogous to vertical fractures. Recent, more realistic techniques involve the use of numerical models. Analysis of horizontal wells using type curve matching was first invented by Thompson and Temeng [18]. Lately, the main trend observed is to apply the convolution and deconvolution method. The convolution method includes the simultaneous operation of both downhole flow-rate and bottomhole pressure measurements to rectify for variations of bottomhole pressure as a result of flow-rate fluctuations throughout a drawdown test. Meanwhile, the deconvolution method converts variation in pressure measurements to a constant rate initial drawdown test and is actually a total least squares nonlinear problem [19].

CHAPTER 3: METHODOLOGY

3.1. RESEARCH METHODOLOGY

This project began with the selection and understanding of project topic. In this study, the main objective is to generate type curves using Matlab software for the purpose of pressure transient analysis of horizontal wells in an anisotropic, rectangular-shaped bounded reservoir with both gas cap and aquifer present as vertical boundaries. The reservoir is bounded horizontally by no-flow boundaries.

The type curves are created based on dimensionless pressure and pressure derivative which are defined in Al Rbeawi and Tiab's study [5]. The type curves will be generated based on equations which the author developed/formulated as adapted from the results of previous analytical technique of Green's function developed by Gringarten and Ramey [1].

As thoroughly analysed by Gringarten and Ramey, through the usage of the Green's function method, it is possible to rigorously articulate the solution of the second order partial differential equation, together with the prescribed boundary conditions, for fluid flow in porous media. The basic concept of this technique is to find the Green's function, under the prescribed boundary conditions, for the partial differential equation. The solution, for such a boundary value problem, can be expressed in terms of an integral equation based on the Green's function obtained. The assumption of uniform flux (fluid withdrawal rate) is used over the source volume. Under the initial conditions of uniform pressure field and outer boundary conditions of either constant pressure or no-flow, there is only one term involved in the expression of the solution (the integral term of the wellbore domain), if we evaluate pressure drop instead of pressure. Since no discretization in the reservoir domain is required, this method is favourable for solving problems with complex 3D-flow geometries.

Other data from literature [5, see Appendices] for pressure drawdown are also obtained to be solved using the proposed type curves for analysis purposes. The type curves are validated against other works in literature [5]. Results are then carefully examined and documented in subsequent reports.

3.2. FLOW PROCESS OF PROJECT WORK

According to the planned timeframe, this project is expected to be completed within 8 months. The following flowchart below details a step-by-step procedure for accomplishing this project.

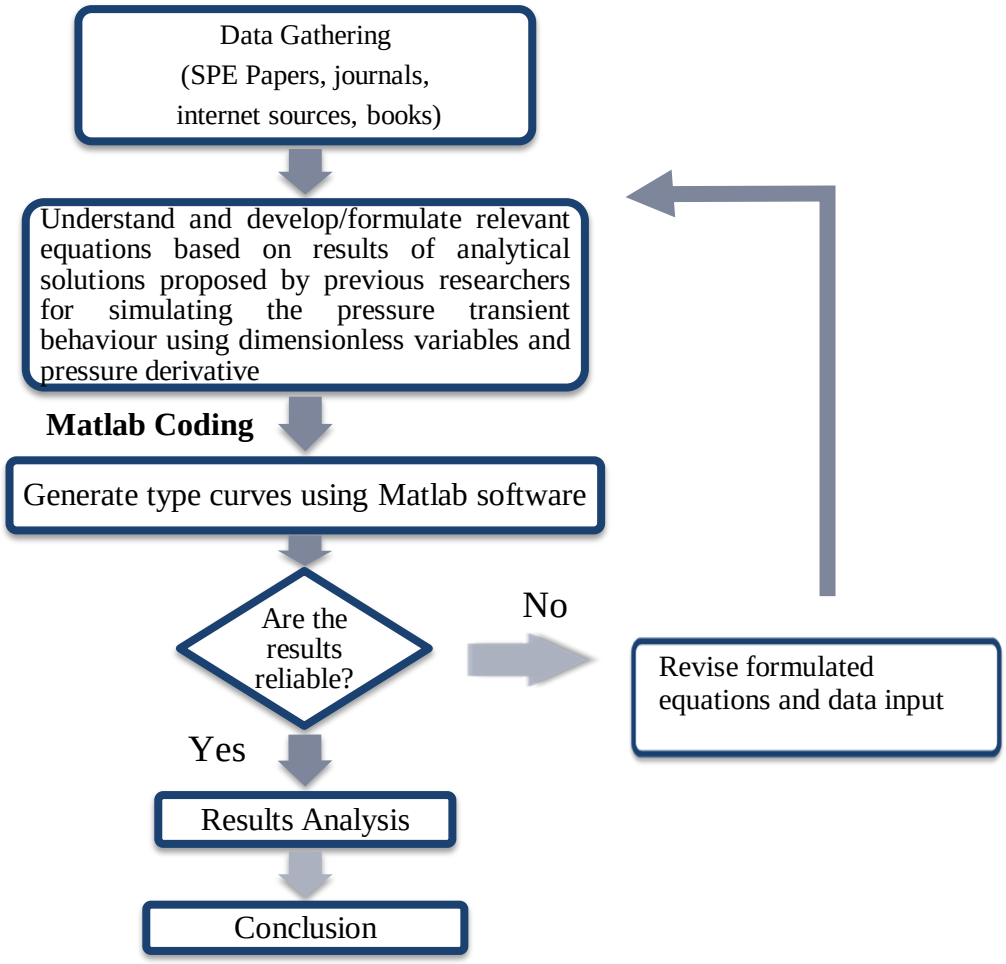

Figure 1: Flowchart of Project Activities

3.3. KEY MILESTONE

Project Milestone	Week No.	Date
Formulating / Developing Equations	13	12/4/15
Matlab Coding	16	1/5/15
Program Validation	20	5/7/15
Generate Type Curves	21	12/7/15
Analysis	23	22/7/15

3.4. GANTT CHART OF PROJECT TIMELINE

Gantt Chart	PERIOD OF PLANNING (WEEKS)																												
Description of Planning	1	2	3	4	5	6	7	8	9	10	11	12	13	14	15	16	17	18	19	20	21	22	23	24	25	26	27	28
Study and select the scope of studies																												
Data Gathering/ Literature Review																												
Submission of Extended Proposal																												
Develop/formulate equations																												
Proposal Defence																												
Learning Software																												
Generate Type Curves with Matlab software																												
Submission of Interim Report																												
Resource Collection																												
Project execution continues																												
Validation of work																												
Analyse the results and discussion																												
Preparation Progress Report																												
Progress Repot Submission																												
Pre-SEDEX Preparation																												
Pre-SEDEX																												
Preparation of Final Report																												
Submission of Draft Final Report																												
Submission of Dissertation (soft copy)																												
Submission of Technical Paper																												
Viva																												
Submission of Project Dissertation (hard copy)																												

CHAPTER 4: RESULTS AND DISCUSSION

The mathematical model as developed below can be used to simulate pressure behaviour created by the horizontal well acting on a reservoir with constant production bounded by gas cap and aquifer and laterally, by no-flow boundaries, as shown in *Figure 2* below. The model below comprises of three instantaneous source solutions as formulated from the results of Gringarten and Ramey's work [1].The dimensionless variables are defined through Al Rbeawi and Tiab's analysis [5]. In applying the theory of Green's function to unsteady flow problems, the introduction of source functions is most convenient by integrating the Green's function over the volume of the source.

4.1. Mathematical Model

The instantaneous Green's function which corresponds to the solution is expressed as the product:

$$S(M,t) = X(x)_{xw=0} VII(y)_{yw=0} VIII(z)_{ze=h}$$

Equation 1: Product of Green's Functions

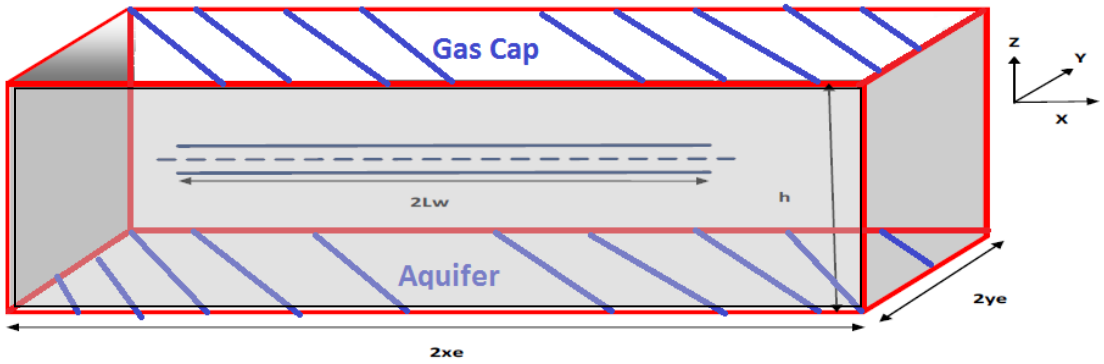

Figure 2 : Horizontal well bounded by vertical constant pressure boundaries and laterally by no-flow boundaries

Firstly, the diffusivity equation describing transient flow of slightly compressible fluid in an anisotropic, homogeneous and porous medium, bounded by a surface S_e can be written as follows:

$$\eta_x \frac{\partial^2 p(M,t)}{\partial x^2} + \eta_y \frac{\partial^2 p(M,t)}{\partial y^2} + \eta_z \frac{\partial^2 p(M,t)}{\partial z^2} - \frac{\partial p(M,t)}{\partial t} = 0$$

Equation 2: Diffusivity Equation

The diffusivity constants are expressed as:

$$\eta_j = \frac{k_j}{\phi \mu c}, \quad j = x, y, z \text{ or } r$$

Equation 3: Diffusivity Constants

Pressure drop can then be expressed as follows:

$$\Delta p(M,t) = \frac{q}{2Lw\emptyset c_t} \int_0^t S(M,\tau) d\tau$$

$$\Delta p(M,t) = \frac{q}{2Lw\emptyset c_t} \int_0^t S(x,\tau) S(y,\tau) S(z,\tau) d\tau$$

Equation 4: Pressure drop

Equation 4 above represents the pressure drop created at point M of infinite extent by an instantaneous point source P; with strength q (q symbolises the quantity of fluid withdrawn from or injected into the reservoir at point P). The strength q can be a function of time and source location. Consequently, based on Lord Kelvin's and Newman's product method in solving 3D heat conduction problems, when the reservoir is not considered to be of infinite extent in all directions, having straight boundaries that

are maintained either as no-flow or constant pressure boundaries (or mixed), the bounded reservoir can be replaced by an infinite reservoir in all directions by taking images in the bounding planes [1]. Hence, the solution of a three dimensional problem can be solved as equivalent to the product of solutions of three one dimensional problems.

Next, the dimensionless pressure is defined, along with all the other supplementary dimensionless variables as listed here from Al Rbeawi and Tiab's study [5]:

$$P_D(x_D, y_D, z_D, z_{wD}, L_D, t_D) = \frac{2\pi\sqrt{k_x k_y}\, h\, \Delta P}{q\,\mu}$$

$$x_D = \frac{x - x_w}{L_w} \qquad x_{wD} = \frac{x_w}{x_e} \qquad t_D = \frac{k_x t}{\phi\,\mu\, c_t L_w^2} = \frac{\eta_x t}{L_w^2}$$

$$y_D = \frac{y - y_w}{L_w}\sqrt{\frac{k_x}{k_y}} \qquad y_{wD} = \frac{y_w}{y_e} \qquad \text{where } \eta_x = \frac{k_x}{\phi\mu c_t}$$

$$z_D = \frac{z - z_w}{L_w}\sqrt{\frac{k_x}{k_z}} \qquad z_{wD} = \frac{z_w}{h} \qquad L_D = \frac{L_w}{h}\sqrt{\frac{k_z}{k_x}}$$

$$z_{wD} = \frac{z_w}{h} \qquad x_{eD} = \frac{L_w}{x_e}$$

$$\bar{z}_D = \frac{z - z_w}{h} = z_D L_D \qquad y_{eD} = \frac{L_w}{y_e}\sqrt{\frac{k_y}{k_x}}$$

Substituting pressure drop, ΔP (*Equation 4*) into the dimensionless pressure equation gives us:

$$P_D(x_D, y_D, z_D, z_{wD}, L_D, t_D) = \frac{2\pi\sqrt{k_x k_y}\, h}{q\,\mu} \quad \frac{q}{2Lw\phi c_t} \int_0^t S(x,\tau)S(y,\tau)S(z,\tau)d\tau$$

$$P_D(x_D, y_D, z_D, z_{wD}, L_D, t_D) = \frac{\pi\sqrt{k_x k_y}h}{Lw\emptyset c_t \quad \mu} \int_0^t S(x,\tau)S(y,\tau)S(z,\tau)d\tau$$

Equation 5: Dimensionless Pressure equation without tD

Incorporating the definition of dimensionless time (tD) into the above equation (Equation 5), gives us *Equation 6* as stated below:

$$t_D = \frac{k_x t}{\phi \mu c_t L_w^2} = \frac{\eta_x t}{L_w^2}$$

$$P_D(x_D, y_D, z_D, z_{wD}, L_D, t_D) = \frac{\pi\sqrt{k_x k_y}h}{Lw\emptyset c_t \mu} \frac{\phi \mu c_t L_w^2}{k_x} \int_0^{t_D} S(x_D,\tau_D)S(y_D,\tau_D)S(z_D,\tau_D)d\tau$$

$$P_D(x_D, y_D, z_D, z_{wD}, L_D, t_D) = \pi\sqrt{\frac{k_x}{k_y}}\, h\, Lw \int_0^{t_D} S(x_D,\tau_D)S(y_D,\tau_D)S(z_D,\tau_D)d\tau$$

Equation 6: Dimensionless Pressure (pD) equation incorporated with Dimensionless Time (tD)

Thereafter, defining the source functions for all three directions as represented below for pressure transient behaviour of horizontal wells in a reservoir bounded vertically by constant pressure boundaries and laterally by no-flow boundaries:

$$S(x,t)=\frac{L_w}{x_e}\left[1+\frac{4x_e}{\pi L_w}\sum_{n=1}^{\infty}\frac{1}{n}\exp\left(-\frac{\pi^2 n^2 \eta_x t}{4x_e^2}\right)\sin\left(n\pi\frac{L_w}{2x_e}\right)\cos\left(n\pi\frac{x_w}{2x_e}\right)\cos\left(n\pi\frac{x}{2x_e}\right)\right]$$

Equation 7: Source function in x direction

When converted to dimensionless variables, each term inside the bracket corresponds to:

$\exp\left(-\frac{\pi^2 n^2 \eta_x^2 t}{4x_e^2}\right)$	$X_{eD}^2 \tau_D = \frac{Lw^2}{Xe^2} * \frac{\eta_x t}{Lw^2} = \frac{\eta_x t}{x_e{}^2}$
$\left\|\sin\left(n\pi\frac{L_w}{2x_e}\right)\right\|$	$X_{eD} = \frac{Lw}{Xe}$
$\cos\left(n\pi\frac{x_w}{2x_e}\right)$	$X_{wD} = \frac{X_w}{X_e}$
$\cos\left(n\pi\frac{x}{2x_e}\right)$	$X_D X_{eD} + X_{wD} = \frac{x - x_w}{Lw} * \frac{Lw}{x_e} + \frac{x_w}{x_e} = \frac{x}{xe}$

Hence, the complete dimensionless equation for the x-direction is:

$$S(X_D,\tau_D)=\frac{Lw}{Xe}\left[1+\frac{4}{\pi x_{eD}}\sum_{n=1}^{\infty}\frac{1}{n}\exp\left(-\frac{\pi^2 n^2 x_{eD}^2 \tau_D}{4}\right)\sin\left(n\pi\frac{x_{eD}}{2}\right)\cos\left(n\pi\frac{x_{wD}}{2}\right)\cos\left(\frac{n\pi}{2}(x_D x_{eD}+x_{wD})\right)\right]$$

Equation 8: Dimensionless equation for source function in x-direction

Equation 9: Source function in y direction

$$S(y,t)=\frac{1}{2y_e}\left[1+2\sum_{n=1}^{\infty}\exp(-\frac{\pi^2 n^2 \eta_y t}{4y_e^2})\cos(n\pi\frac{y_w}{2y_e})\cos(n\pi\frac{y}{2y_e})\right]$$

When converted to dimensionless variables, each term inside the bracket corresponds to:

$$\boxed{\tau_D=\frac{\eta_x t}{Lw^2}} \quad \text{where } \eta_x=\frac{k_x}{\phi\mu c_t} \qquad \boxed{\frac{K_y=\eta_y\phi\mu c_t}{K_x=\eta_x\phi\mu c_t}=\frac{\eta_y}{\eta_x}}$$

$$\exp(-\frac{\pi^2 n^2 \eta_y t}{4y_e^2}) \quad \Big| \quad y_{eD}^2\tau_D=\frac{Lw^2}{Ye^2}*\left(\sqrt{\frac{ky}{kx}}\right)^2\frac{\eta_x t}{Lw^2}$$

$$=\frac{Lw^2}{Ye^2}\frac{ky}{kx}*\frac{\eta_x t}{Lw^2}$$

$$=\frac{Lw^2}{Ye^2}\frac{\eta_y}{\eta_x}*\frac{\eta_x t}{Lw^2}$$

$$=\frac{\eta_y t}{y_e^2}$$

$$\cos(n\pi\frac{y_w}{2y_e}) \quad \Big| \quad y_{wD}=\frac{Y_w}{Y_e}$$

$$\cos(n\pi\frac{y}{2y_e}) \quad \Big| \quad Y_{DY}Y_{eD}+Y_{wD}=\frac{y-y_w}{Lw}\sqrt{\frac{ky}{kx}}*\frac{Lw}{y_e}\sqrt{\frac{kx}{ky}}+\frac{y_w}{y_e}=\frac{y}{y_e}$$

Hence, the complete dimensionless equation for the y-direction is :

$$\boxed{S(Y_D,\tau_D)=\frac{1}{2y_e}\left[1+2\sum_{n=1}^{\infty}\exp(-\frac{\pi^2 n^2 y_{eD}^2\tau_D}{4})\cos(n\frac{y_{wD}}{2})\cos(\frac{n\pi}{2}(y_D y_{eD}+y_{wD}))\right]}$$

Equation 10: Dimensionless equation for source function in y-direction

Equation 11: Source function in z direction:

$$S(z,t) = \frac{2}{h} \sum_{n=1}^{\infty} \exp\left(-\frac{\pi^2 n^2 \eta_z^2 t}{h^2}\right) \sin\left(n\pi \frac{z_w}{h}\right) \sin\left(n\pi \frac{z}{h}\right)$$

When converted to dimensionless variables, each term inside the bracket corresponds to:

$\exp\left(-\frac{\pi^2 n^2 \eta_z^2 t}{h^2}\right)$

$$L_D = \frac{L_w}{h}\sqrt{\frac{k_z}{k_x}} \qquad L_D{}^2 \times \tau_D$$

$$\tau_D = \frac{\eta_x t}{L_w{}^2}$$

$$L_D = \frac{L_w}{h}\sqrt{\frac{\eta_z \emptyset \mu C_t}{\eta_x \emptyset \mu C_t}} \qquad L_D{}^2 \times \tau_D = \frac{L_w{}^2}{h^2}\frac{\eta_z}{\eta_x} \times \frac{\eta_x t}{L_w{}^2}$$

$$L_D = \frac{L_w}{h}\sqrt{\frac{\eta_z}{\eta_x}} \qquad L_D{}^2 \times \tau_D = \frac{\eta_z t}{h^2}$$

$$L_D{}^2 = \frac{L_w{}^2}{h^2}\left(\sqrt{\frac{\eta_z}{\eta_x}}\right)^2$$

$$L_D{}^2 = \frac{L_w{}^2}{h^2}\frac{\eta_z}{\eta_x}$$

$\sin\left(n\pi \frac{z_w}{h}\right)$

$$\frac{z_w}{h} = z_{wD}$$

$$z_D L_D = \frac{z - z_w}{L_w}\sqrt{\frac{k_x}{k_z}} \times \frac{L_w}{h}\sqrt{\frac{k_z}{k_x}}$$

$\sin\left(n\pi \frac{z}{h}\right)$

$$z_D L_D = \frac{z - z_w}{h}$$

$$z_D L_D + z_{wD} = \frac{z - z_w}{h} + \frac{z_w}{h} = \frac{z}{h}$$

Hence, the complete dimensionless equation for the z-direction is:

$$S(Z_D, \tau_D) = \frac{2}{h} \sum_{n=1}^{\infty} \exp(-n^2 \pi^2 L_D^2 \tau_D) \sin(n\pi z_{wD}) \sin(n\pi(z_D L_D + z_{wD}))$$

Equation 12: Dimensionless equation for source function in z-direction

Combining all equations together into the dimensionless pressure equation:

$$P_D(x_D, y_D, z_D, z_{wD}, L_D, t_D) = \pi \sqrt{\frac{k_x}{k_y}}\, h\, Lw \int_0^{t_D} S(x_D, \tau_D) S(y_D, \tau_D) S(z_D, \tau_D) d\tau$$

$$P_D(x_D, y_D, z_D, z_{wD}, L_D, t_D) = \pi \sqrt{\frac{k_x}{k_y}}\, h\, Lw \; \frac{Lw}{Xe} \frac{1}{2y_e} \frac{2}{h} \int_0^{tD} \left[1 + \frac{4}{\pi x_{eD}} \sum_{n=1}^{\infty} \frac{1}{n} \exp\left(-\frac{\pi^2 n^2 x_{eD}^2 \tau_D}{4}\right) \sin\left(n\pi \frac{x_{eD}}{2}\right) \cos\left(n\pi \frac{x_{wD}}{2}\right) \cos\left(\frac{n\pi}{2}(x_D x_{eD} + x_{wD})\right) \right] \times$$

$$\left[\sum_{n=1}^{\infty} \exp\left(-\frac{\pi^2 n^2 y_{eD}^2 \tau_D}{4}\right) \cos\left(n \frac{y_{wD}}{2}\right) \cos\left(\frac{n\pi}{2}(y_D y_{eD} + y_{wD})\right) \right] \times$$

$$\left[\sum_{n=1}^{\infty} \exp(-n^2 \pi^2 L_D^2 \tau_D) \sin(n\pi z_{wD}) \sin(n\pi(z_D L_D + z_{wD})) \right]$$

$$P_D(x_D, y_D, z_D, z_{wD}, L_D, t_D) = \pi \frac{Lw}{Xe} \frac{Lw}{y_e} \sqrt{\frac{k_x}{k_y}} \int_0^{tD} \left[1 + \frac{4}{\pi x_{eD}} \sum_{n=1}^{\infty} \frac{1}{n} \exp\left(-\frac{\pi^2 n^2 x_{eD}^2 \tau_D}{4}\right) \sin\left(n\pi \frac{x_{eD}}{2}\right) \cos\left(n\pi \frac{x_{wD}}{2}\right) \cos\left(\frac{n\pi}{2}(x_D x_{eD} + x_{wD})\right) \right] \times$$

$$\left[\sum_{n=1}^{\infty} \exp\left(-\frac{\pi^2 n^2 y_{eD}^2 \tau_D}{4}\right) \cos\left(n \frac{y_{wD}}{2}\right) \cos\left(\frac{n\pi}{2}(y_D y_{eD} + y_{wD})\right) \right] \times$$

$$\left[\sum_{n=1}^{\infty} \exp(-n^2 \pi^2 L_D^2 \tau_D) \sin(n\pi z_{wD}) \sin(n\pi(z_D L_D + z_{wD})) \right]$$

$$P_D = \pi \cdot X_{eD} Y_{eD} \int_0^{tD} \left[1 + \frac{4}{\pi x_{eD}} \sum_{n=1}^{\infty} \frac{1}{n} \exp\left(-\frac{\pi^2 n^2 x_{eD}^2 \tau_D}{4}\right) \sin\left(n\pi \frac{x_{eD}}{2}\right) \cos\left(n\pi \frac{x_{wD}}{2}\right) \cos\left(\frac{n\pi}{2}(x_D x_{eD} + x_{wD})\right) \right] \times$$

$$\left[\sum_{n=1}^{\infty} \exp\left(-\frac{\pi^2 n^2 y_{eD}^2 \tau_D}{4}\right) \cos\left(n \frac{y_{wD}}{2}\right) \cos\left(\frac{n\pi}{2}(y_D y_{eD} + y_{wD})\right) \right] \times$$

$$\left[\sum_{n=1}^{\infty} \exp(-n^2 \pi^2 L_D^2 \tau_D) \sin(n\pi z_{wD}) \sin(n\pi(z_D L_D + z_{wD})) \right]$$

Equation 13: Result –Final Mathematical Model

4.2. MATLAB Program Verification Procedure

The mathematical model (*Equation 13*) has been coded into the MATLAB software. The parameters in the resulting program have been varied several times, subsequently producing around more than 20 different programs for verification purposes. However, only the significant results and their respective coded programs will be shown and discussed here.

An attempt to verify the MATLAB coded program(s) was conducted mainly against Al Rbeawi and Tiab's work – *Transient Pressure Analysis of Horizontal Wells in a Multi-Boundary System* [5]. Firstly, this is because the dimensionless parameters are defined in the same way as their paper, hence, allowing for faster and more precise verification procedure. However, since Al Rbeawi and Tiab focused on vertical no-flow boundaries while the author's model concentrated on constant pressure boundaries, only *the early times* can be compared and matched for verification purposes (where the boundaries have not affected the pressure behaviour yet). In addition, since the specified reservoir geometry currently under research has not been investigated in the past, verification of the MATLAB program is only limited to early times.

Parameters used in Al Rbeawi and Tiab's work [5]		
Properties	**Nomenclature of Properties**	**Range of Dimensionless Parameters**
h=50	Formation thickness, ft^2	LD=0.1,0.2,0.4 - 40
Lw=800	Half-length of horizontal well, ft	XeD= 0.1 – 1
kx=8	Formation Permeability X direction, mD	YeD= 0.1 – 1
ky=5	Formation Permeability Y direction, mD	ZwD= 0.05,0.1 - 0.5
kz=2	Formation Permeability Z direction, mD	tD=0.33
Xe=2000	Half Distance to boundary X direction,ft	PD=0.078
Ye=2108	Half Distance to boundary Y direction,ft	
Pi=9500	Initial Pressure, psi	
Q=500	Oil Rate, STB/D	
Φ = 0.1	Porosity	
μ = 0.5	Viscosity, cp	
$C_t=2*10^{-6}$	Total Compressibility, 1/psi	
$r_w=0.63$	Wellbore Radius, ft	
B=1.15	Oil Formation Volume Factor, bbl/STB	

Table 1: Parameters used in Al Rbeawi and Tiab's analysis [5]

Variables	Remarks
LD=8	Well distance
XD=0.0001	Pressure measured at production point
YD=0.0001	
ZD=0.00075	
ZwD=0.5	Well located in middle of reservoir height
XwD=0.5	Well located in middle of reservoir, X direction
XeD=0.1 - 1	
YeD=0.1 - 1	

Table 2: Dimensionless Parameters used in Al Rbeawi and Tiab's analysis [5]

As shown here below is the graph for LD=8 (reservoir thickness of 50 ft), for the parameters of XeD=0.1. As can be observed below, the data at early times matches with literature [5] which validates the author's mathematical model.

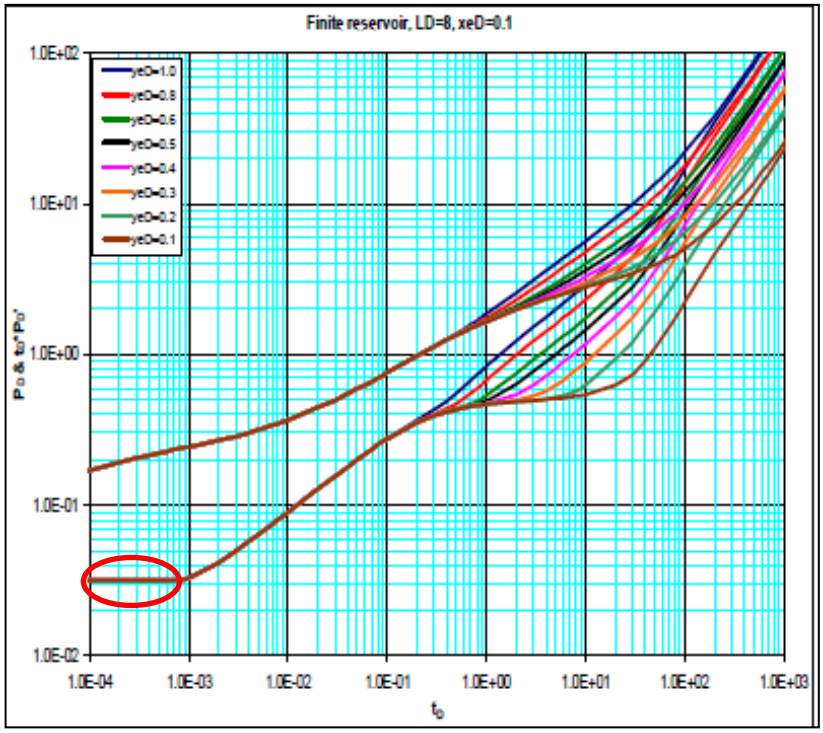

Figure 3: Pressure Behaviour extracted from Al Rbeawi and Tiab's study [5] for the vertical no-flow boundaries, LD=8, XeD=0.1.

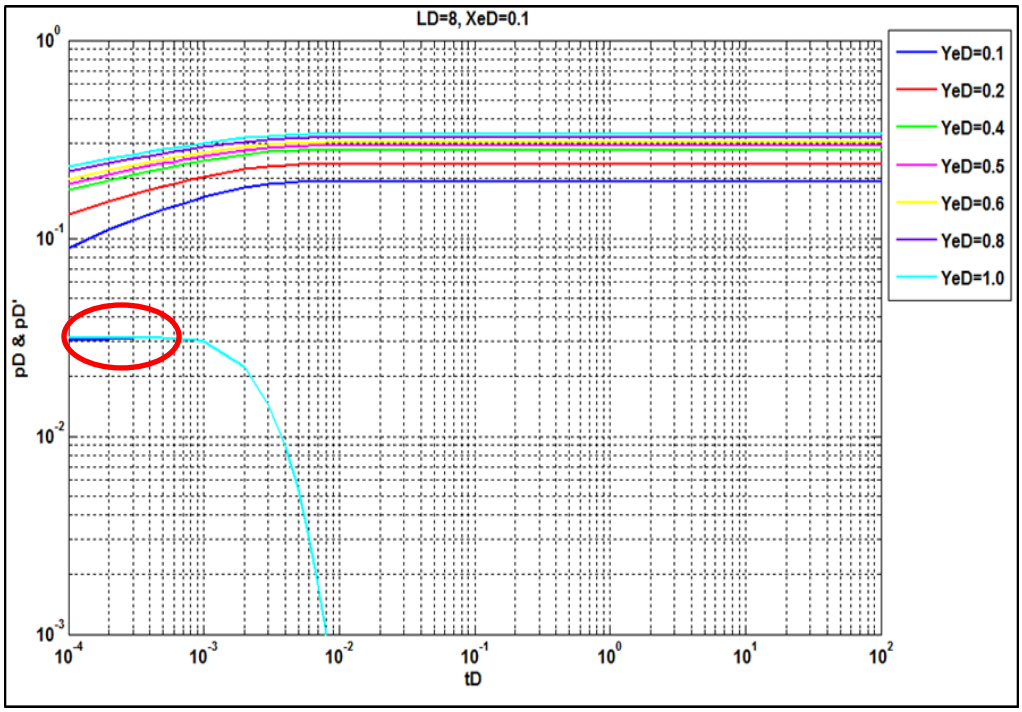

Figure 4: Pressure Behaviour comparison with author's mathematical model against literature [5] for the vertical constant pressure boundaries, LD=8, XeD=0.1.

4.3. Numerical Differentiation

The analytical solution of the pressure derivative coded in the MATLAB program was also verified by calculating the pressure derivative numerically in Excel spreadsheet using the formula below as stated in Horne's book [20], *Modern Well Test Analysis*:

$$t\left[\frac{\partial p}{\partial t}\right]_i = t_i\left[\frac{(t_i - t_{i-1})\,\Delta p_{i+1}}{(t_{i+1} - t_i)\,(t_{i+1} - t_{i-1})} + \frac{(t_{i+1} + t_{i-1} - 2t_i)\,\Delta p_i}{(t_{i+1} - t_i)\,(t_i - t_{i-1})} - \frac{(t_{i+1} - t_i)\,\Delta p_{i-1}}{(t_i - t_{i-1})\,(t_{i+1} - t_{i-1})}\right]$$

Equation 14: Numerical Differentiation

It has been observed by comparing *Figure 4* above and *Figure 5* below; that the trends of the pressure behaviour at early times calculated analytically and numerically matched each other quite well.

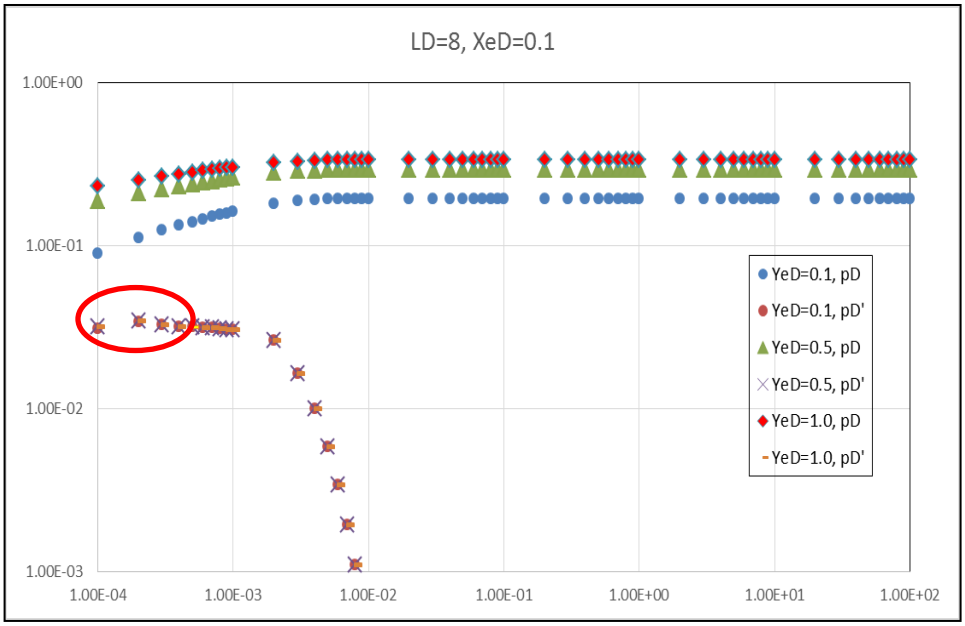

Figure 5: Pressure Behaviour - Numerical Solution for vertical constant pressure boundaries, LD=8, XeD=0.1.

For further sake of verifiying the analytical solution, other specific values taken such as LD=1, XeD=0.5 with varying YeD=0.1 till YeD=1.0 have been extracted.

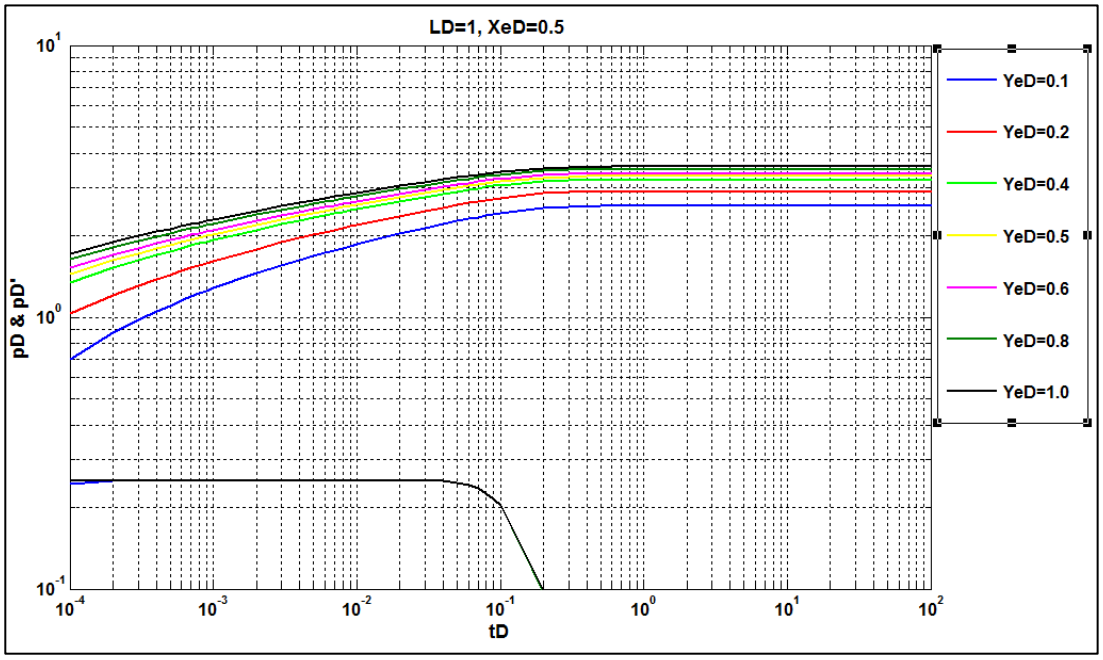

Figure 6: Analytical solution extracted from MATLAB software

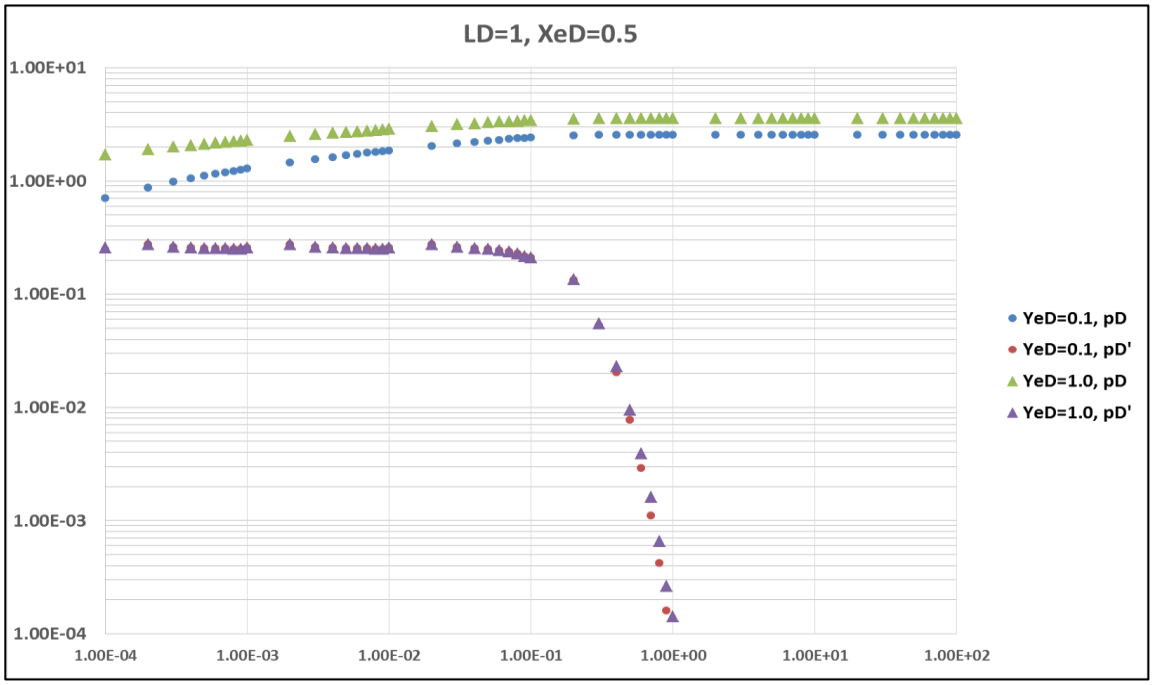

Figure 7: Numerical Integration - plotted in Microsoft Excel

4.4. Pressure Behaviour and Flow Regimes

In a bounded reservoir, generally, the pressure response of horizontal wells acting in finite reservoir with vertical no-flow boundaries exhibits the following five flow regimes:

1. Early Radial Flow
2. Early Linear Flow
3. Pseudo-radial flow
4. Channel Flow (late linear flow)
5. Pseudo-steady state flow

The flow regimes above are displayed through these graphs in the literature [5]:

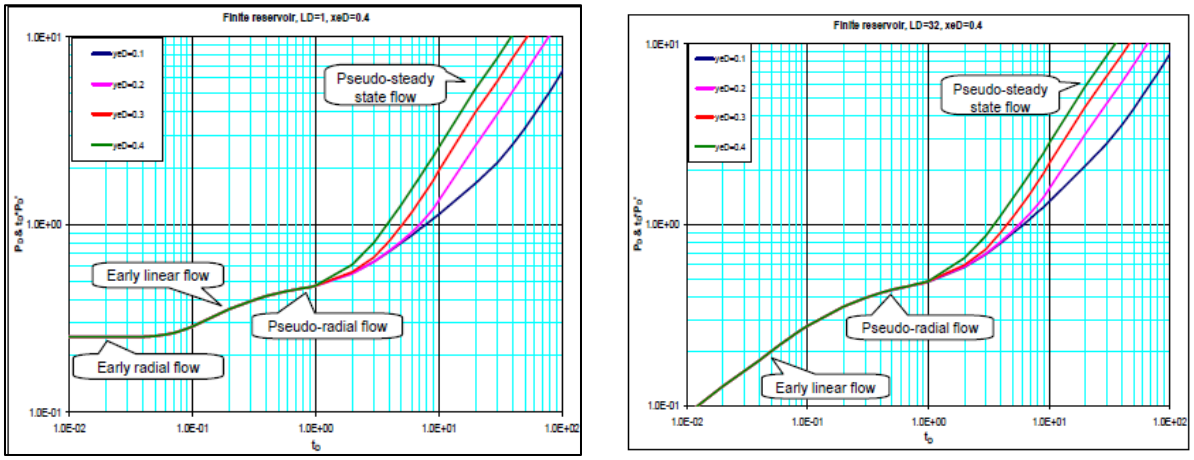

Figure 8: Flow regimes exhibited for different horizontal wells [5]

4.4.1. Early Radial Flow

However, the graphs shown here are based on Al Rbeawi and Tiab's study for reservoir with vertical no-flow boundaries. Meanwhile, the current reservoir geometry studied by the author possesses both gas cap and aquifer. In his study [17], Kuchuk et al. stated that elliptic cylindrical flow is the first pattern before the flow becomes radial. Short time approximation for this flow is defined by Al Rbeawi and Tiab [5] as:

$$t_D = \frac{(1 - x_D)^2}{20}$$

Equation 15: Calculating limit of early radial flow

Based on the results obtained, it can be deduced that all the other flow regimes as mentioned in the literature above [5] are masked by constant pressure behaviour except early radial flow. Thus, only the early radial flow regime and the constant pressure boundary are observed below.

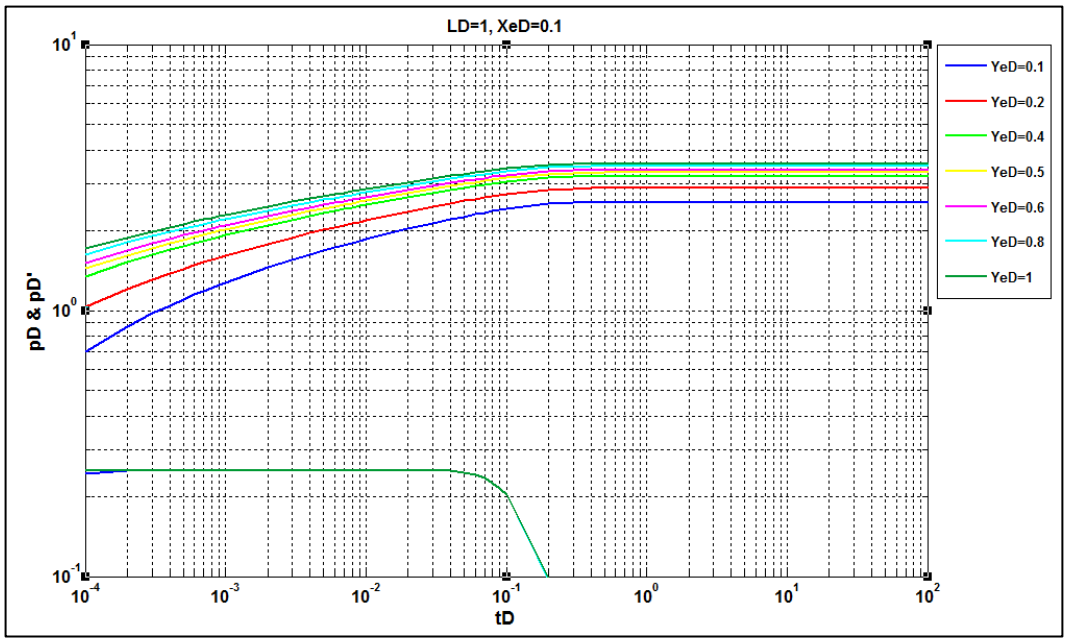

Figure 9: Flow regimes exhibited for different horizontal wells, LD=1 (400 ft reservoir thickness)

4.4.2. Visualisation of all other flow regimes

4.4.2.1. Late Linear Flow

Normally, the late linear flow occurs when the pressure have diffused and reached the lateral no-flow boundaries [5, 14, 17]. However, under the realistic physical reservoir thickness, this flow regime could not be observed for the reservoir with vertical constant pressure boundaries. Table 3 below displays the reservoir parameter used in this study.

Table 3: Reservoir Thickness used in this study

Parameter Limit	Reservoir Thickness (ft)	Dimensionless Variable
max	400	LD = 1
min	12	LD = 32

Hence, for the sake of research purposes, the reservoir thickness was varied to 4000 ft. It was discovered that the late linear flow does exist (characterised by a half slope line in the pressure derivative) as illustrated on *Figure 10*.

A minimal value of LD=0.1 was chosen so as to increase the thickness, hypothetically to 4000ft (though *physically unrealistic*) just to enable the visualisation of all the other flow regimes; to allow longer time for the pressure to diffuse before reaching the constant pressure boundaries.

Theoretically, it is deduced that due to the large extent of reservoir thickness, the pressure diffuses faster to the lateral boundaries as opposed to the vertical constant pressure boundaries. Thus, the late linear flow regime appeared before the constant pressure behaviour.

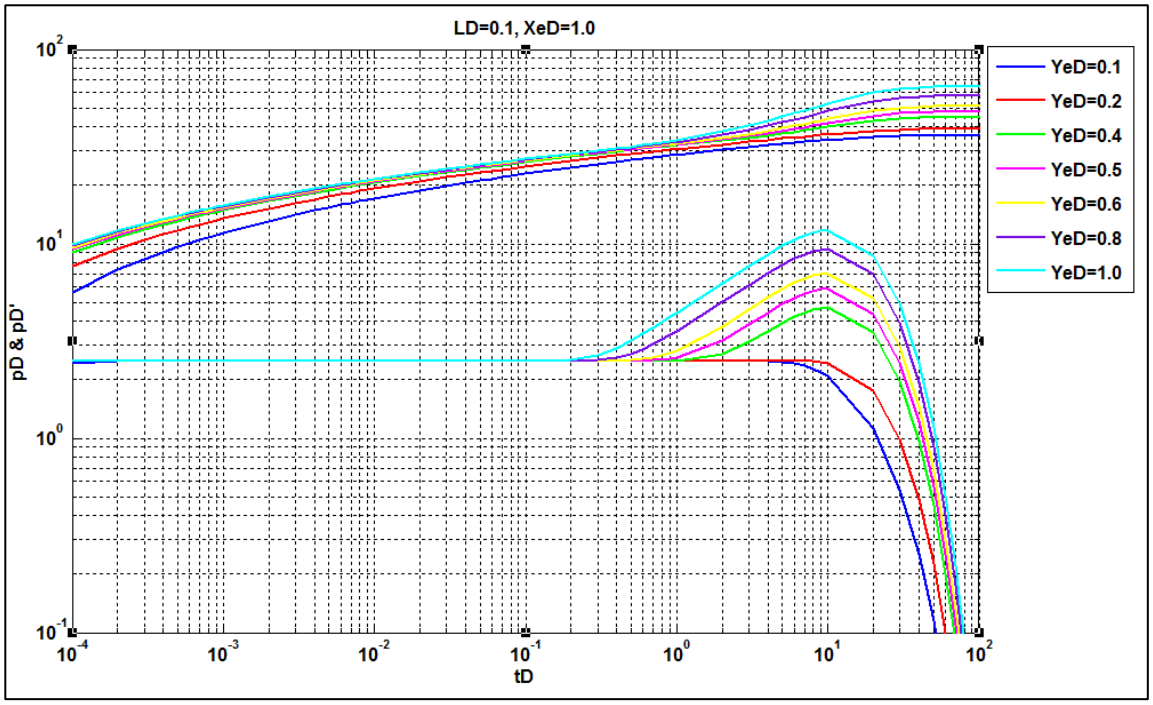

Figure 10: Visualisation of early radial flow, linear flow and constant pressure behaviour, LD=0.1

4.4.2.2. Effects of lateral boundaries

It is observed from the *Figure 10* above that as YeD increases, the linear flow regime could be visualised more clearly. YeD represents the distance to the Y boundary. This indicates a clear relationship with the lateral no-flow boundary in the Y direction as shown mathematically below:

$$y_{eD} = \frac{L_w}{y_e}\sqrt{\frac{k_y}{k_x}}$$

Equation 16: Lateral Boundary to the nearest Y boundary, dimensionless variable

Mathematically, as YeD increases, Ye (distance of the well to the Y-boundary) is shorter and hence, the pressure diffuses faster and linear flow regime could be seen more clearly before effects of vertical constant pressure boundary.

Hence, since, other flow regimes are masked by the constant pressure behaviour using more realistic physical values of LD (example LD>1, 400 ft instead of LD=0.1, 4000 ft), thus, it is concluded that all type curves generated in this study are dominantly focused on only the trends of early radial flow and constant pressure behaviour. The differences in the type curves generated by author are only in the duration of the early radial flow. Hence, for example in *Figure 11* below, it can be observed that as reservoir thickness decreases, the pressure diffuses faster and hence, the early radial flow is masked more quickly by trend of constant pressure behaviour.

Table 4: LD (dimensionless parameters) with respective reservoir thickness

LD	h (ft)
1	400
2	200
4	100
8	50
16	25

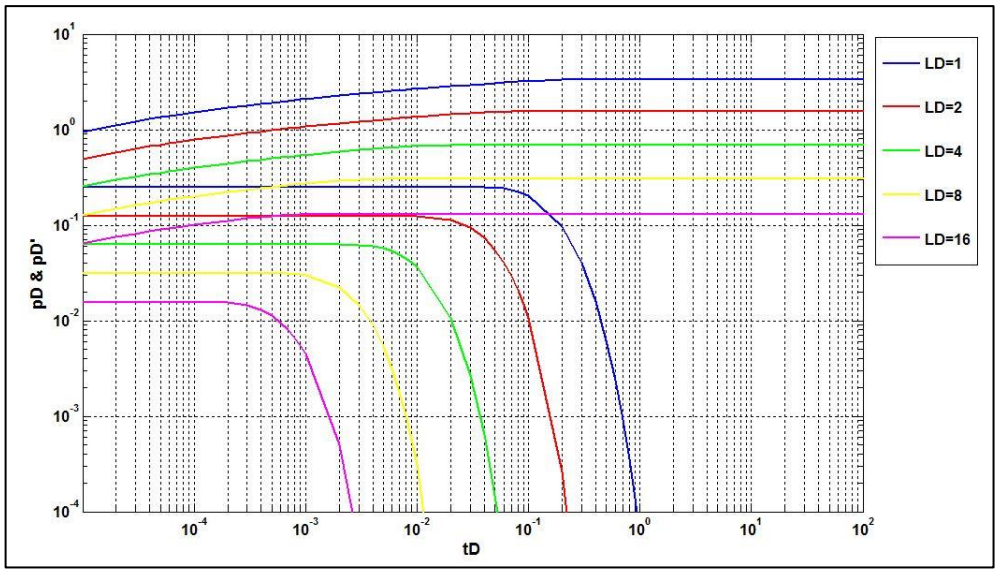

Figure 11: Type curve of short horizontal wells, LD<20

It is deduced based on the type curves generated that varying YeD and XeD (distance to lateral boundaries) do not have significant effect on pressure derivatives; rather only the pressure value changes. This indicates that for the reservoir geometry under study, the pressure derivative is not affected by distance to the boundary in both X and Y directions.

Yet, pressure derivative is only significantly affected by the ratio of the wellbore length to the reservoir thickness (LD). This phenomenon reported actually eases the practice of type curves as users would only need to match with the pressure, since all pressure derivatives are showing same trend/values. The type curves are given in the Appendices.

4.6. Varying ZwD – distance to vertical constant pressure boundaries

The figure below depicts the varying distance to the vertical constant pressure boundaries in order to see its effects on the pressure behaviour.

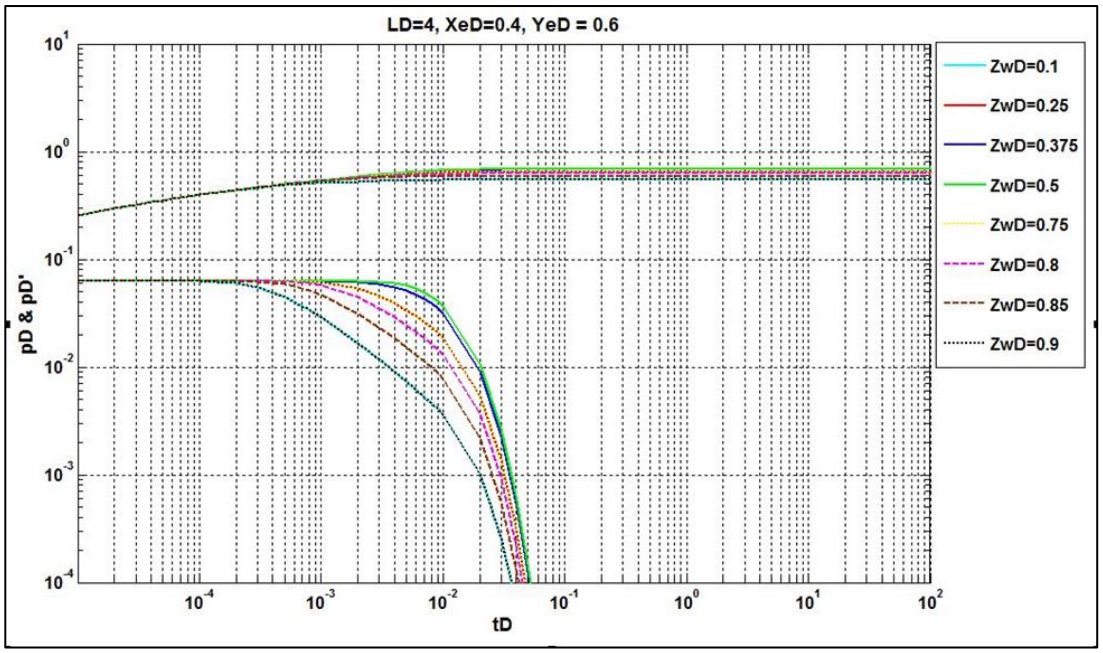

Figure 12: Varying ZwD

It could be seen that, as before, the other flow regimes are masked by constant pressure behaviour. However, varying the ZwD does have the effects on the duration of early radial flow.

For example, if ZwD=0.1, in which the well is closer to the aquifer (aquifer being positioned as Z=0), the early radial flow has shortest duration. The same pressure behaviour occurs if the well is closer to the gas cap (ZwD=0.9). However, as ZwD increases, in which the well is further away from either, or both of the constant pressure boundaries (ZwD=0.5), the early radial flow duration also increases.

4.7. Limitations in this study

The phenomenon as discussed in *section 4.4.2*; which is of the fact that the constant pressure behaviour mask all other flow regimes (except early radial flow) under realistic physical values of reservoir thickness, renders the author unable to generate other interpretation methods based on this reservoir geometry.

Initially in this study, both interpretation techniques of the following (1) Tiab's Direct Synthesis (TDS) – interpreting direct method analytically without type curve matching using log-log plots of the pressure and pressure derivative versus time and secondly, the method of (2) type curve matching were proposed to be conducted.

However, as explained clearly in *section 4.4.2.*, it is only possible for us to observe large reservoir thickness with an unrealistic physical value of LD=0.1, hence, it is concluded that the author will only stick to generating type curves.

4.8. Type Curve Matching Application

As shown on the plots in the appendices, both the pressure and pressure derivative have a unique shape for each combination of the distance to the outer boundaries *Xe* and *Ye* (reservoir configuration). These plots can be used for the type-curve matching technique to determine reservoir characteristics such as: permeability in the three directions and the distance to the boundaries. The following steps adapted from Al Rbeawi and Tiab's paper summarises the procedures required in this technique [5]:

1- Plot (ΔP vs. t) and ($t \times \Delta P'$ vs. t) on log-log paper.
2- Obtain the best match of the data with one of the type curves.
3- Read from any match point: $t_M, \Delta P_M, t_{DM}, P_{DM}, L_D, x_{eDM}, y_{eDM}$.
4- Calculate k_x, k_y, k_z from the following equations:

$$k_x = \frac{\phi \mu c_t L_w^2 t_{DM}}{0.0002637 t_M} \quad (79)$$

$$k_y = \frac{1}{k_x}\left[\frac{141.2 q \mu B P_{DM}}{h \Delta P_M}\right]^2 \quad (80)$$

$$k_z = \left(\frac{L_D^2 h^2}{L_w^{\,2}}\right) k_x \quad (81)$$

5- Calculate x_e using:

$$x_e = \frac{L_w}{x_{eDM}} \quad (82)$$

6- Calculate y_e using:

$$y_e = \frac{L_w}{y_{eDM}} \sqrt{\frac{k_y}{k_x}} \quad (83)$$

II. EXAMPLE

A pressure drawdown test data of a horizontal well acting on a finite reservoir are given in Table B-1 of Appendix (B). Other known reservoir and well data are:

$q = 500$ STB/D $\quad \phi = 0.1$ $\quad \mu = 0.5$ cp

$c_t = 2\text{x}10^{-6}$ psi^{-1} $\quad B = 1.15$ bbl/STB $\quad h = 50$ ft

$L = 1600$ ft $\quad r_w = 0.63$ ft $\quad p_i = 9500$ psi

Estimate formation permeability in all direction and the distance to the outer boundaries.

III. SOLUTION

1-The pressure and pressure derivative plot is shown in **Fig. (17)**.

2- The matching process is shown in **Fig. (18)**.

3- Read from the matching point:

$$t_M = 10,\ t_{DM} = 0.33,\ \Delta P_M = 10,\ P_{DM} = 0.078,\ L_{DM} = 8,\ x_{eDM} = 0.4,\ y_{eDM} = 0.3$$

4- The permeabilities in the x, y, z directions from Eqs. (79, 80, 81):

$$k_x = \frac{0.1 \times 0.5 \times 0.00002 \times 800^2 \times 0.33}{0.0002637 \times 10} = 8\ md$$

$$k_y = \left[\frac{141.2 \times 500 \times 0.5 \times 1.15 \times 0.078}{\sqrt{8} \times 50 \times 10}\right]^2 = 5\ md$$

$$k_H = \sqrt{k_x k_y} = \sqrt{8 \times 5} = 6.3\ md$$

$$k_z = k_V = \frac{8^2 \times 50^2 \times 8}{800^2} = 2\ md$$

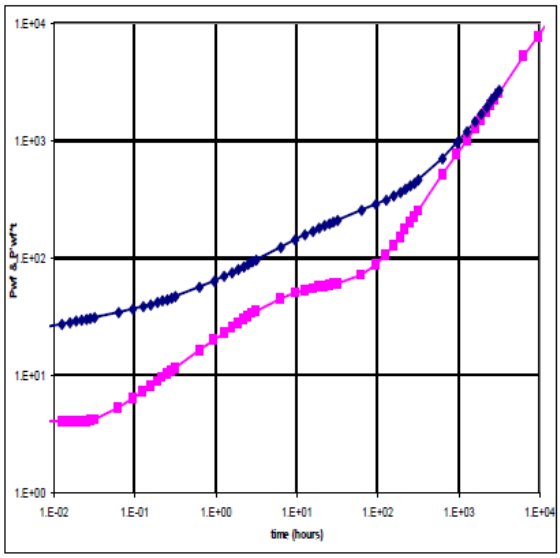

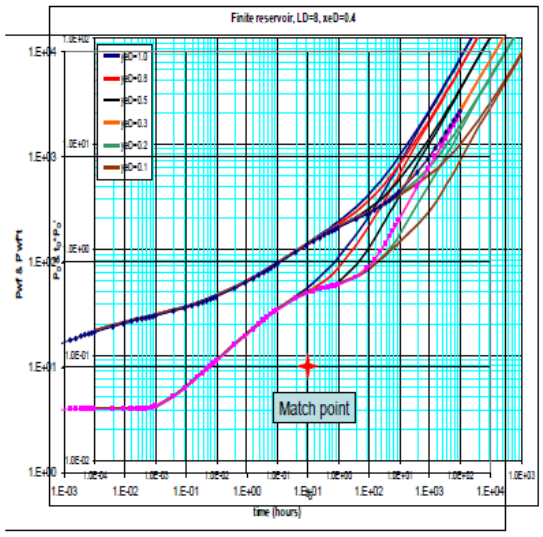

5-The distance to the boundary in the x-direction using Eq. (82):

$$x_e = \frac{800}{0.4} = 2000\ ft$$

6-The distance to the boundary in the y-direction using Eq. (83):

$$y_e = \frac{800}{0.3}\sqrt{\frac{5}{8}} = 2108\ \ ft$$

The above results can be compared with the results obtained by the conventional semilog method as follow:

1- The Cartesian plot of ΔP vs. $\sqrt{t}$, as shown in **Fig. (19)**, yields a straight line corresponding to the early linear flow data. This slope of this line $m_{EL} = 41$ can be used to obtain k_y using Eq. (66):

$$k_y = \left[\frac{8.128 \times 500 \times 1.15}{1600 \times 41 \times 50}\right]^2 \frac{0.5}{0.1 \times 0.000002} = 5\ md$$

2 - From early time data, the semi-log plot of the early radial flow, as shown in **Fig. (20)**, can be used to obtain k_z from the slope of the straight line $m_{ER} = 9.3$ using Eq. (62).

$$k_z = \left[\frac{162.6 \times 0.5 \times 500 \times 1.15}{9.3 \times 1600 \times \sqrt{5}}\right]^2 = 2\ md$$

3- From late time data, the semi-log plot of the pseudo-radial flow as shown in **Fig. (21)** can be used to obtain k_x from the slope of the straight line $m_{PR} = 147$ using Eq. (72).

$$k_x = \left[\frac{162.6 \times 500 \times 0.5 \times 1.15}{147 \times 50 \times \sqrt{5}}\right]^2 = 8\ md$$

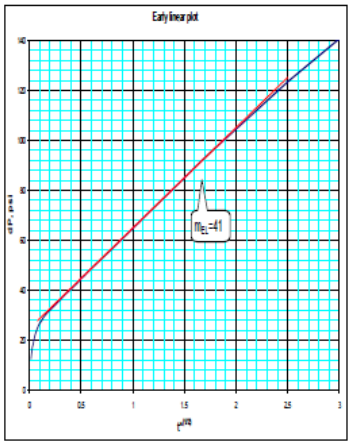

Fig. (19): Early-Linear plot

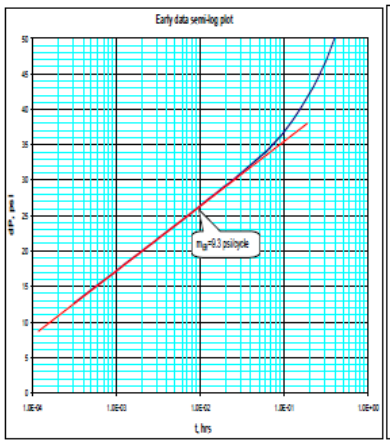

Fig. (20): Early-radial plot.

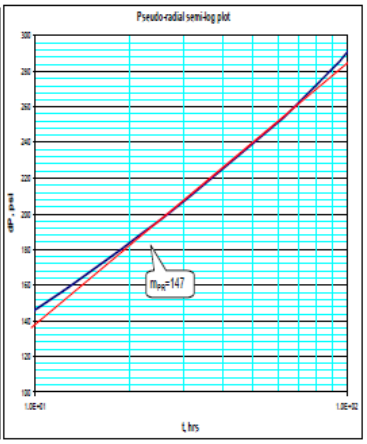

Fig. (21): Pseudo-Radial plot.

CHAPTER 5: CONCLUSION

Many comprehensive analytical solutions for horizontal wells have been proposed in the literature including, Laplace, Fourier transforms and Green's function for both isotropic and anisotropic reservoirs. Using these solutions and dimensionless variables, it is possible to generate pressure and pressure derivative type curves for varying horizontal well parameters. Non-linear least squares estimation is highly recommended for analysing well test data with large number of parameters [17].

Applications of these solutions to several reservoirs with varieties of boundaries have been well studied, especially for the no-flow boundaries. However, not much research was conducted to investigate the transient pressure behaviour for horizontal wells in reservoirs bounded by constant pressure boundaries apart from the research conducted by Lu [2] and Stewart and Du [3] while others such as Kuchuk et al [17] analysed mixed boundaries. Yet, the research studies above [2, 3] still did not consider completely bounded reservoir geometry. This study is hence carried out to investigate effects of both gas cap and aquifer in an anisotropic bounded rectangular-shaped reservoir. Other research studies may have focused on bounded reservoir geometry in all three directions but concentrated on vertical no-flow boundaries [4] – [6].

It is concluded based on this study that:

1. Pressure behavior and flow regimes of horizontal wells acting in bounded reservoirs are affected significantly by the outer boundaries.
2. The impact of the boundaries on pressure responses and fluid flow regimes occur at late time production. Pressure behaviors and flow regimes at early time production are not affected by the boundaries.
3. Only early radial flow and constant pressure behaviour could be mainly observed in this study. Expected flow regimes commonly occurring in horizontal well testing are masked by the effects of constant pressure behaviour. Only when reservoir thickness is increased significantly, do we see other common flow regimes.

4. When LD=0.1, reservoir thickness very big, channel flow usually occurs for the following cases:
    - The distance to one of the boundaries is significantly smaller than the second boundary.
    - The wellbore penetrates completely the formation in the long horizontal direction.
5. The pressure behavior of the long horizontal well, i.e. LD>20, is similar to the behavior of vertical fractures. Early radial flow can't be seen for long horizontal wells.
6. Permeabilities in all three directions and well location with respect to the boundaries can be estimated using type curve matching technique.

REFERENCES

[1] A. C. Gringarten and H. J. Ramey Jr, "The use of source and Green's functions in solving unsteady-flow problems in reservoirs," *SPE Journal*, vol. 13, pp. 285-296, 1973.

[2] J. Lu, "A Mathematical Model of Horizontal Wells Productivity and Well Testing Analysis," Virginia Polytechnic Institute and State University, 1998.

[3] K.-F. Du and G. Stewart, "Analysis of Transient Pressure Response of Horizontal Wells in Bounded Reservoirs Using Derivative Approach," 1994/3/1/ 1994.

[4] F. Daviau, G. Mouronval, G. Bourdarot, and P. Curutchet, "Pressure analysis for horizontal wells," SPE Formation Evaluation, vol. 3, pp. 716-724, 1988.

[5] S. J. H. Al Rbeawi and D. Tiab, "Transient Pressure Analysis of Horizontal Wells in a Multi-Boundary System," in *SPE Production and Operations Symposium*, 2013.

[6] L. C. Wang Xiaodong, "Horizontal Well Pressure Analysis In Box-Bounded Reservoirs," *Appl. Math. Mech. -Engl. Ed.*, vol. 19, pp. 315-320, 1998-04-18 1998.

[7] A. B. Newman, "Heating and cooling rectangular and cylindrical solids," *Industrial & Engineering Chemistry*, vol. 28, pp. 545-548, 1936

[8] P. Goode and R. Thambynayagam, "Pressure drawdown and buildup analysis of horizontal wells in anisotropic media," *SPE Formation Evaluation*, vol. 2, pp. 683-697, 1987.

[9] F. Giger, "Theoretical Evaluation of the Effect of Water Cresting on Production by Horizontal Wells "*Revue de l'inst. Francais du Petrole*, 1983.

[10] D. Spivak, *Pressure Analysis for Horizontal Wells*: Louisiana Tech University, 1988.

[11] J. Striegler, "Arco finishes fourth horizontal drainhole," *Oil Gas Journal ;(United States)*, vol. 80, 1982.

[12] A. Chaudhry, *Oil Well Testing Handbook*. Houston, Texas: Gulf Professional

Publishing: Elsevier, 2004.

[13] SPE International. (2014, December 15). *Horizontal Wells*. [Online]. Available: http://petrowiki.org/Horizontal_wells

[14] J. Lee, J. B. Rollins, and J. P. Spivey, *Pressure transient testing*: Richardson, Tex.: Henry L. Doherty Memorial Fund of AIME, Society of Petroleum Engineers, 2003.

[15] M. D. Clonts and H. Ramey Jr, "Pressure transient analysis for wells with horizontal drainholes," in *SPE California Regional Meeting*, 1986.

[16] W. Thomson and B. Kelvin, "Mathematical and Physical Papers," *Bull. Amer. Math. Soc. 20 (1914), 431-432 DOI: http://dx. doi. org/10.1090/S0002-9904-1914-02527-3 PII*, pp. 0002-9904, 1914.

[17] F. Kuchuk, P. Goode, D. Wilkinson, and R. Thambynayagam, "Pressure-transient behavior of horizontal wells with and without gas cap or aquifer," *SPE Formation Evaluation*, vol. 6, pp. 86-94, 1991.

[18] L. G. Thompson and K. O. Temeng, *Automatic Type-Curve Matching for Horizontal Wells*: Society of Petroleum Engineers, 1993.

[19] T. Von Schroeter, F. Hollaender, and A. C. Gringarten, *Deconvolution of Well Test Data as a Nonlinear Total Least Squares Problem*: Society of Petroleum Engineers, 2001.

[20] Horne, R. N. *Modern Well Test Analysis*. Petroway Inc, 1995.

APPENDICES

Table 5: Pressure Drawdown Data extracted from Al Rbeawi and Tiab's study for verification purposes [5]

t, hrs	Pwf, psi	t, hrs	Pwf, psi	t, hrs	Pwf, psi	t, hrs	Pwf, psi
0	9500	0.031533	9469.02	6.306661	9376.40	945.9992	8544.48
0.000315	9487.42	0.063067	9465.85	9.459992	9357.07	1261.332	8296.37
0.000631	9484.69	0.0946	9463.55	12.61332	9342.22	1576.665	8048.00
0.000946	9483.11	0.126133	9461.62	15.76665	9330.16	1891.998	7799.44
0.001261	9481.96	0.157667	9459.92	18.91998	9320.01	2207.331	7550.73
0.001577	9481.06	0.1892	9458.39	22.07331	9311.24	2522.665	7301.91
0.001892	9480.33	0.220733	9456.97	25.22665	9303.50	2837.998	7052.98
0.002207	9479.71	0.252266	9455.66	28.37998	9296.59	3153.331	6803.97
0.002523	9479.18	0.2838	9454.42	31.53331	9290.32	6306.661	4311.03
0.002838	9478.70	0.315333	9453.26	63.06661	9246.18	9459.992	1815.31
0.003153	9478.28	0.630666	9443.83	94.59992	9215.33		
0.006307	9475.50	0.945999	9436.59	126.1332	9188.42		
0.00946	9473.87	1.261332	9430.49	157.6665	9162.94		
0.012613	9472.72	1.576665	9425.12	189.1998	9137.99		
0.015767	9471.82	1.891998	9420.28	220.7331	9113.24		
0.01892	9471.09	2.207331	9415.83	252.2665	9088.56		
0.022073	9470.47	2.522665	9411.72	283.7998	9063.91		
0.025227	9469.94	2.837998	9407.87	315.3331	9039.25		
0.02838	9469.45	3.153331	9404.26	630.6661	8792.19		

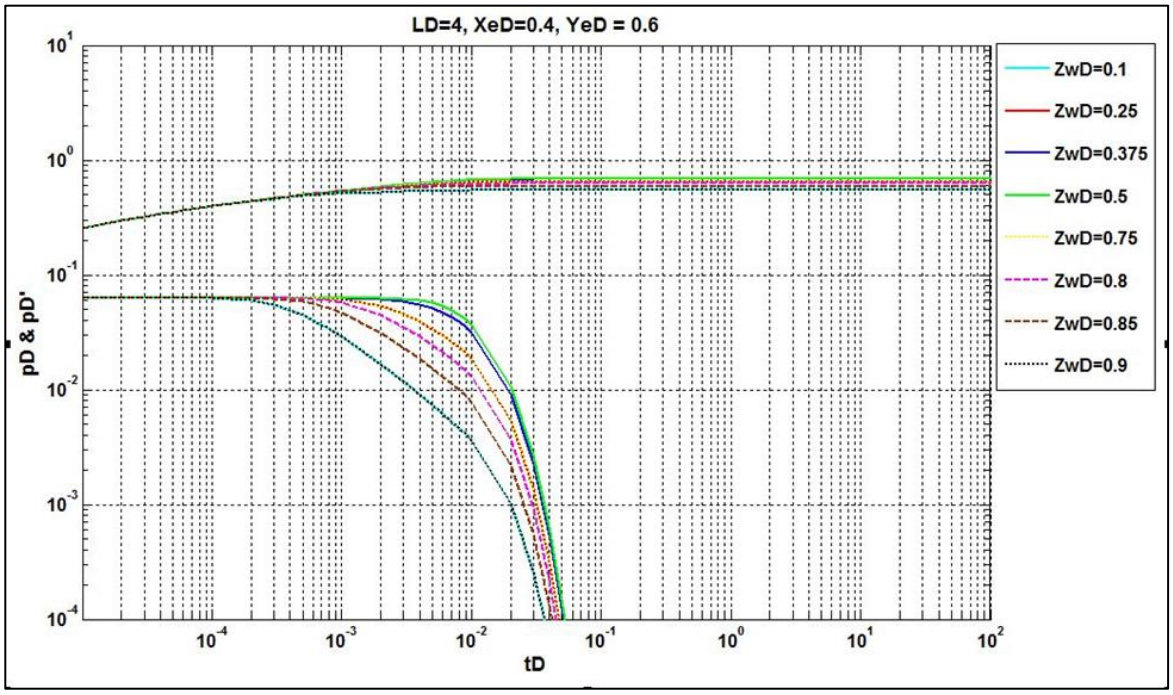

Figure 13: Pressure Behaviour - effect from varying the thickness (distance to vertical constant pressure boundaries)

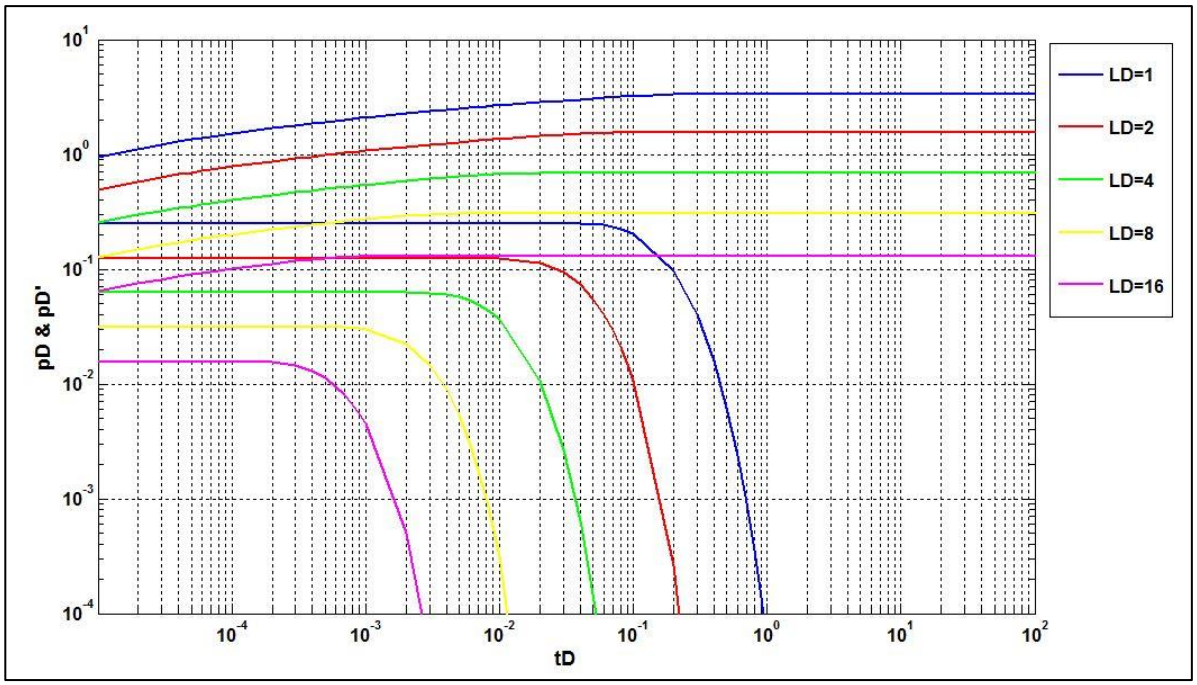

Figure 14: Type curves for short horizontal wells, LD<20 (shorter wells as compared to reservoir thickness), XeD=0.4, YeD=0.6

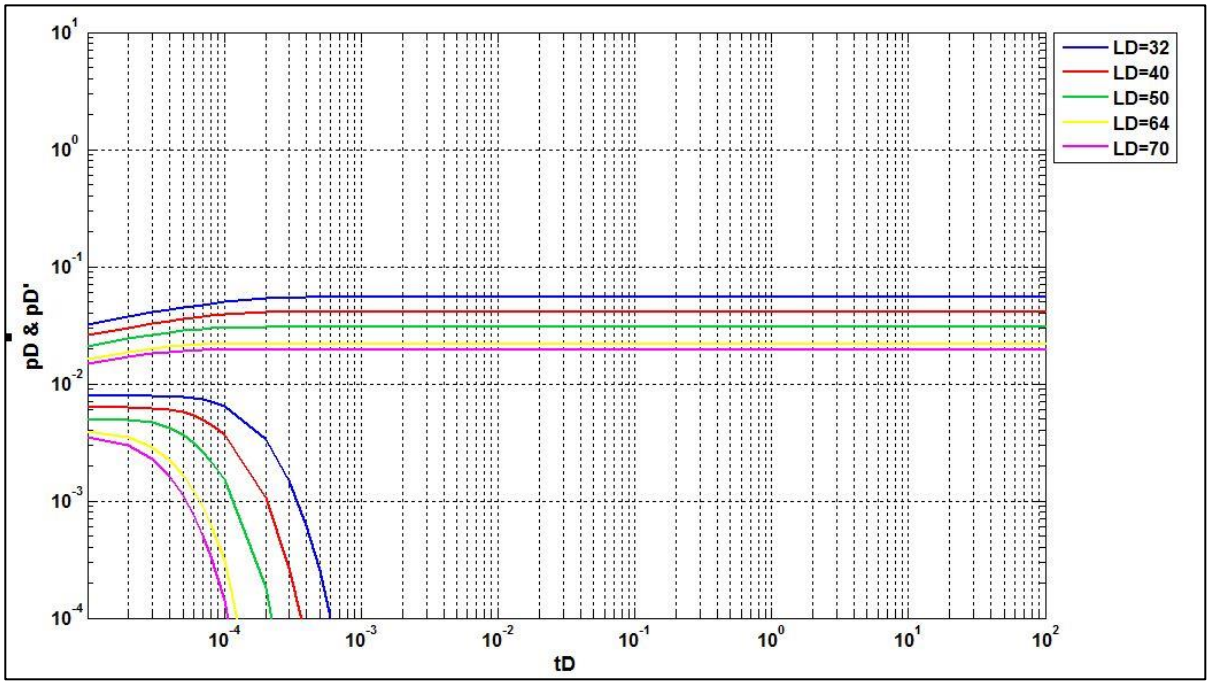

Figure 15: Type curves for long horizontal wells, LD>20 (longer wells as compared to reservoir thickness), XeD=0.4, YeD=0.6

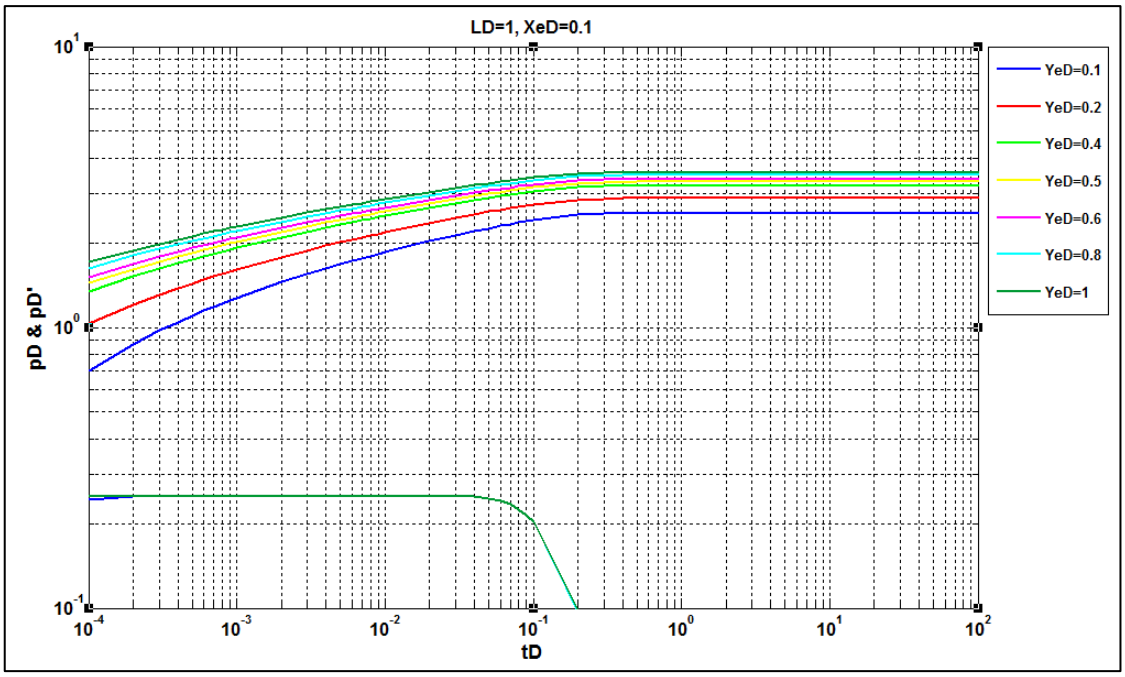

Figure 16: Type curve for short horizontal well, LD=1, XeD=0.1

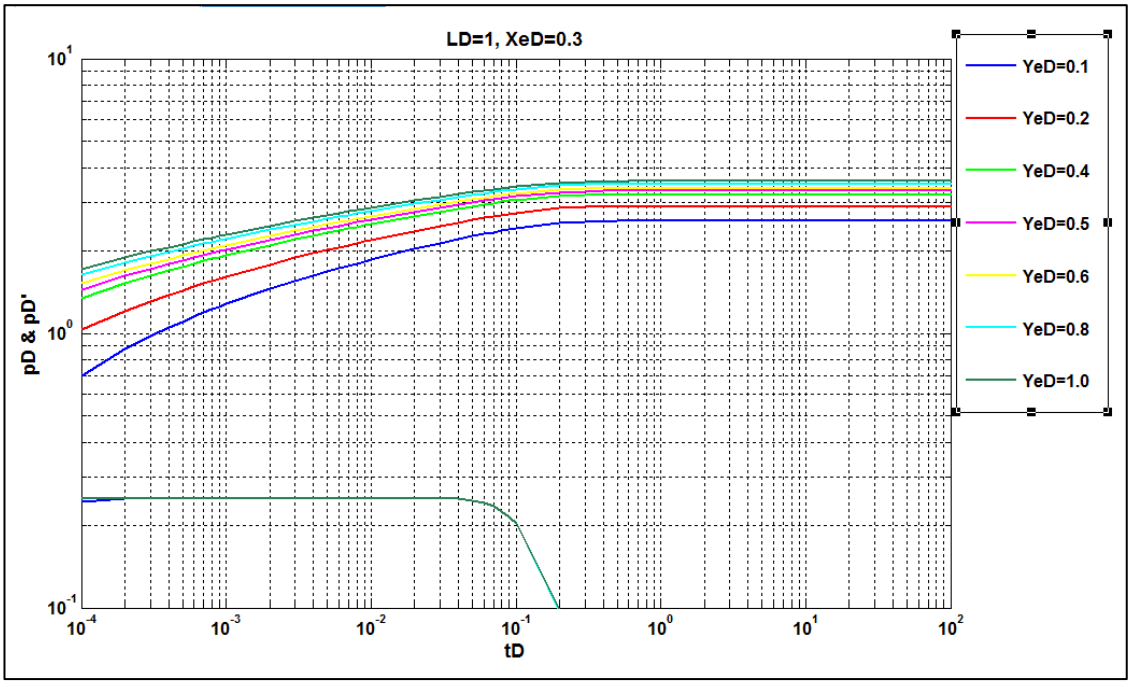

Figure 17: Type curve for short horizontal well, LD=1, XeD=0.3

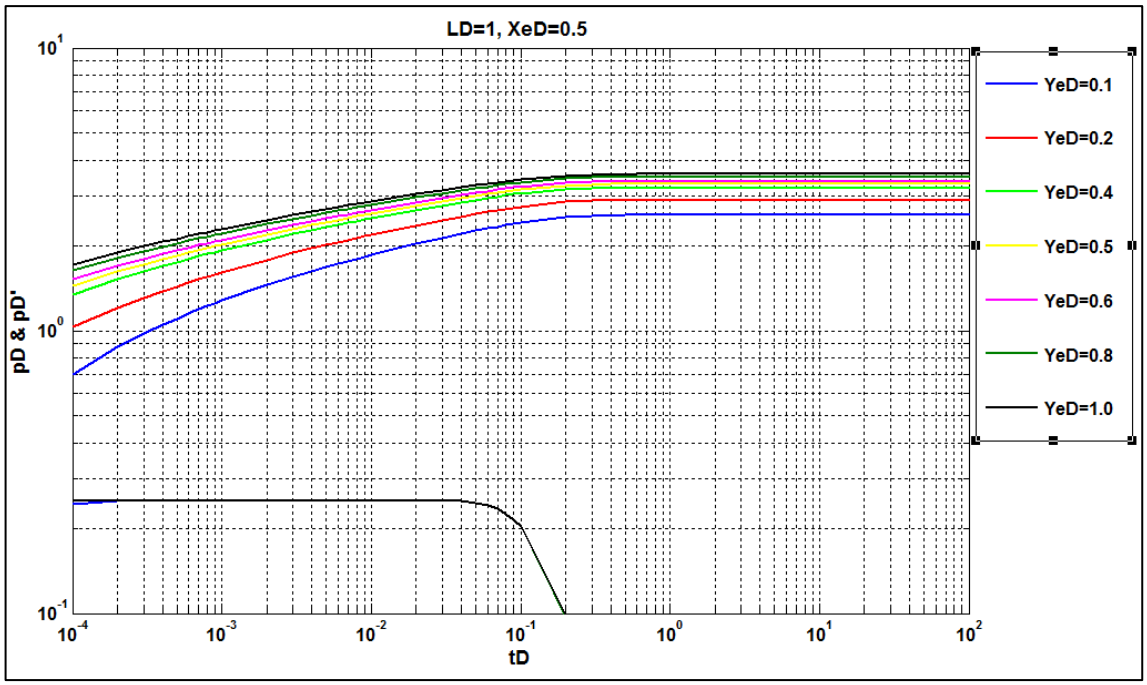

Figure 18: Type curve for short horizontal well, LD=1, XeD=0.5

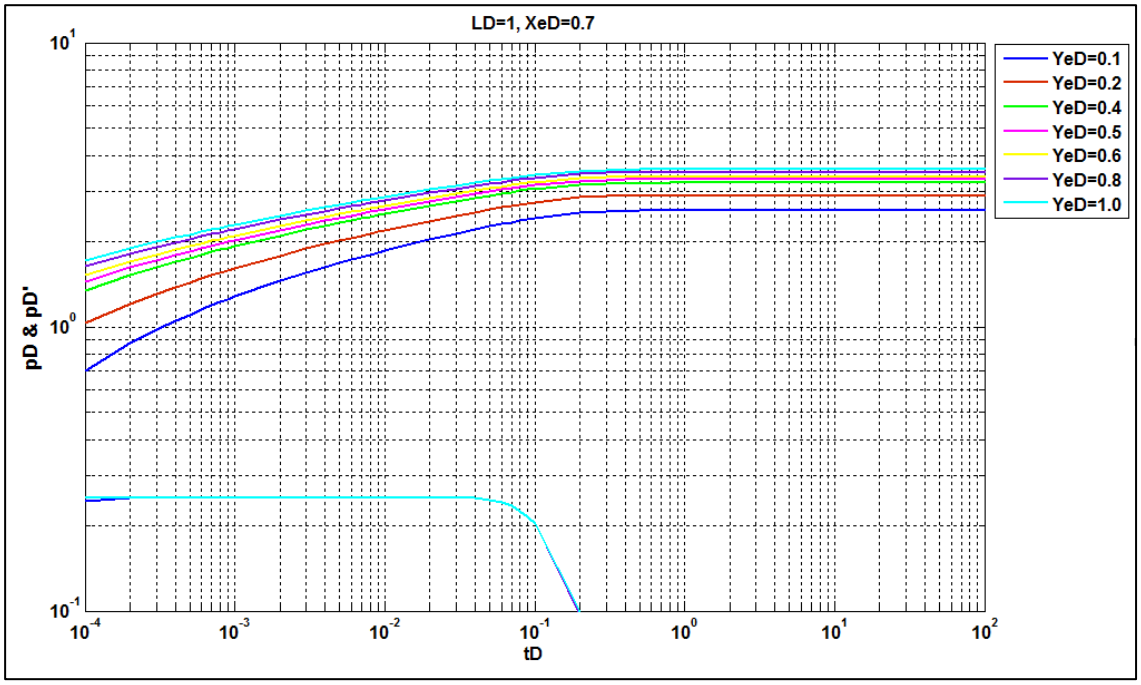

Figure 19: Type curve for short horizontal well, LD=1, XeD=0.7

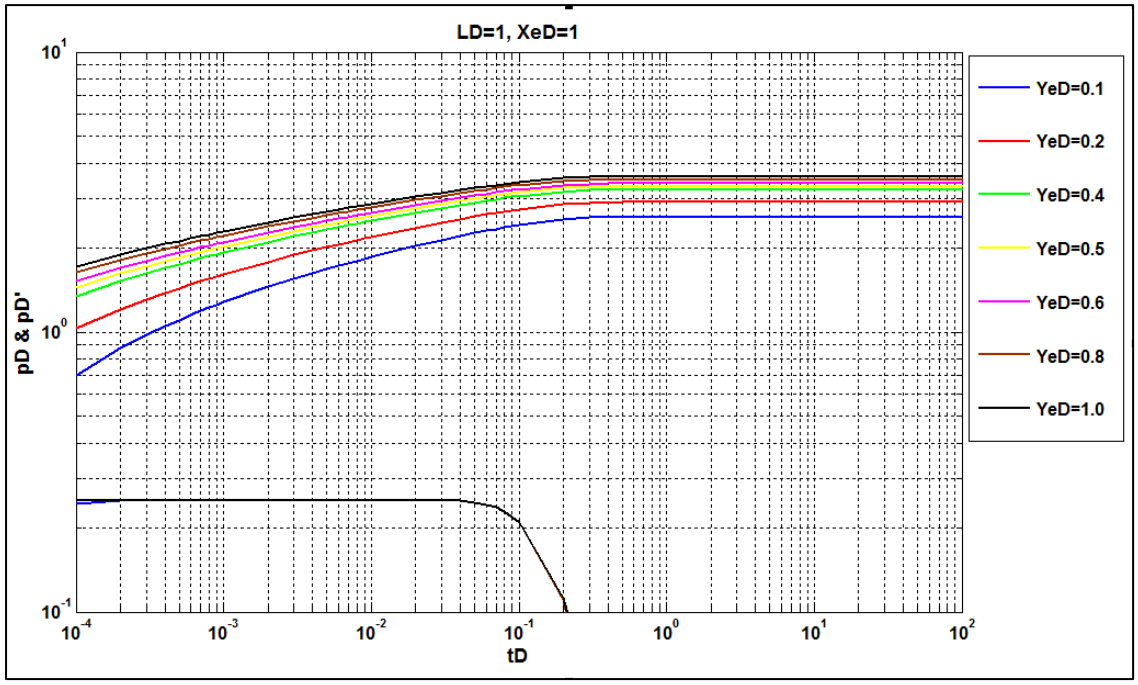

Figure 20: Type curve for short horizontal well, LD=1, XeD=1.0

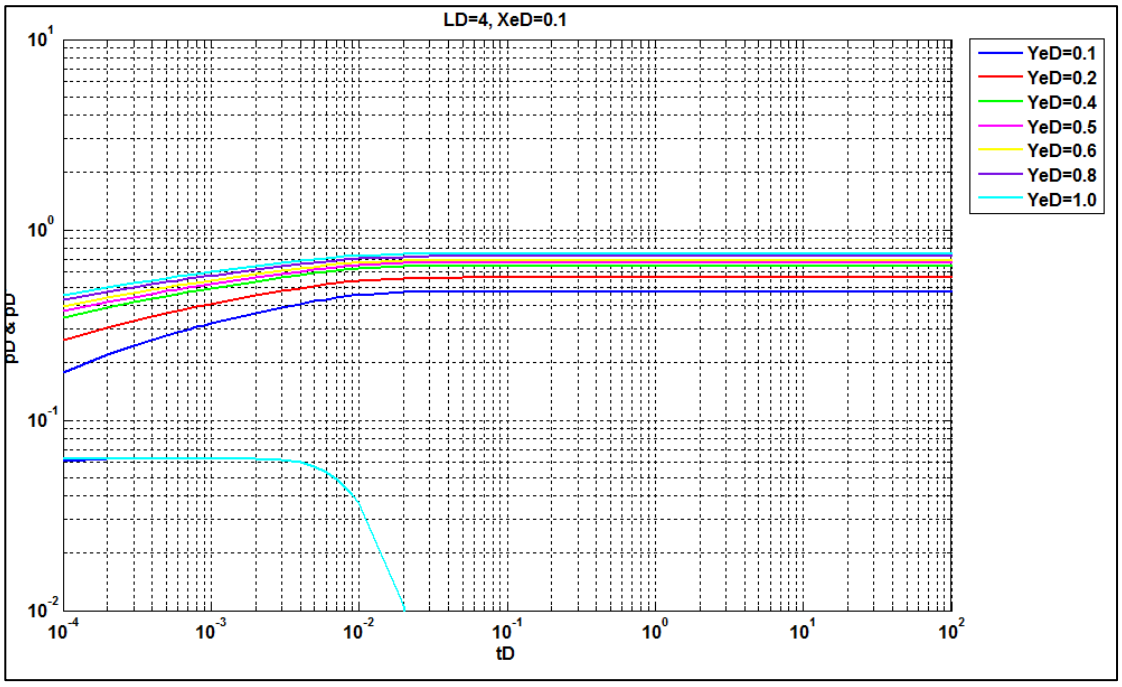

Figure 21: Type curve for short horizontal well, LD=4, XeD=0.1

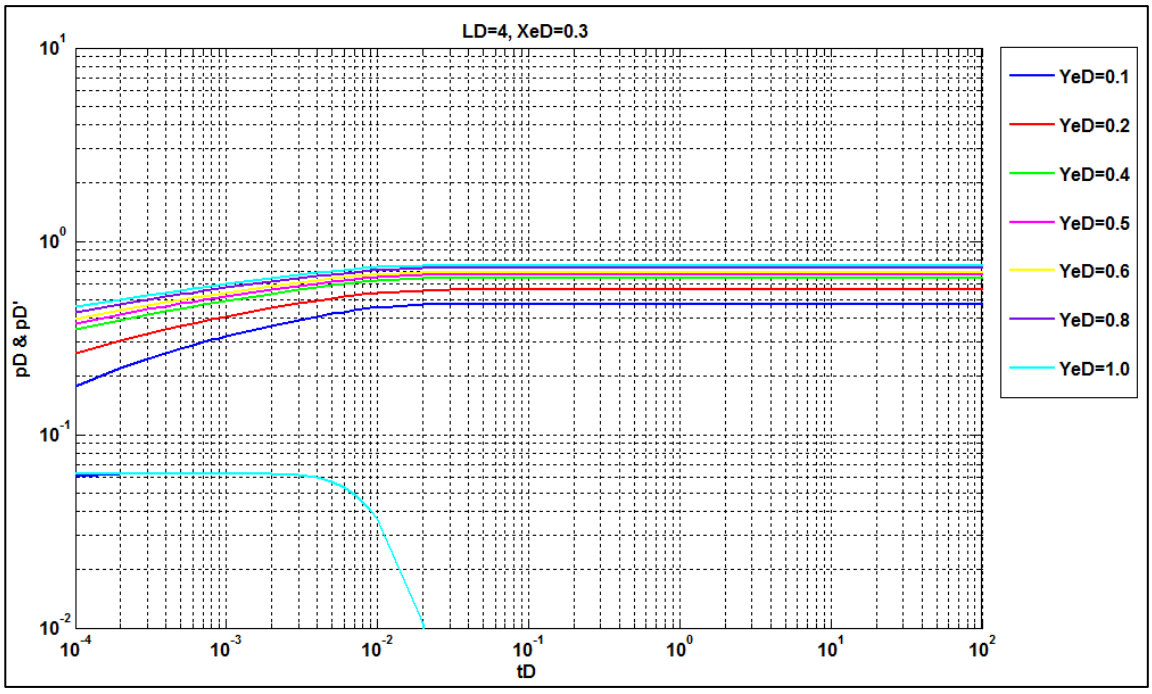

Figure 22: Type curve for short horizontal well, LD=4, XeD=0.3

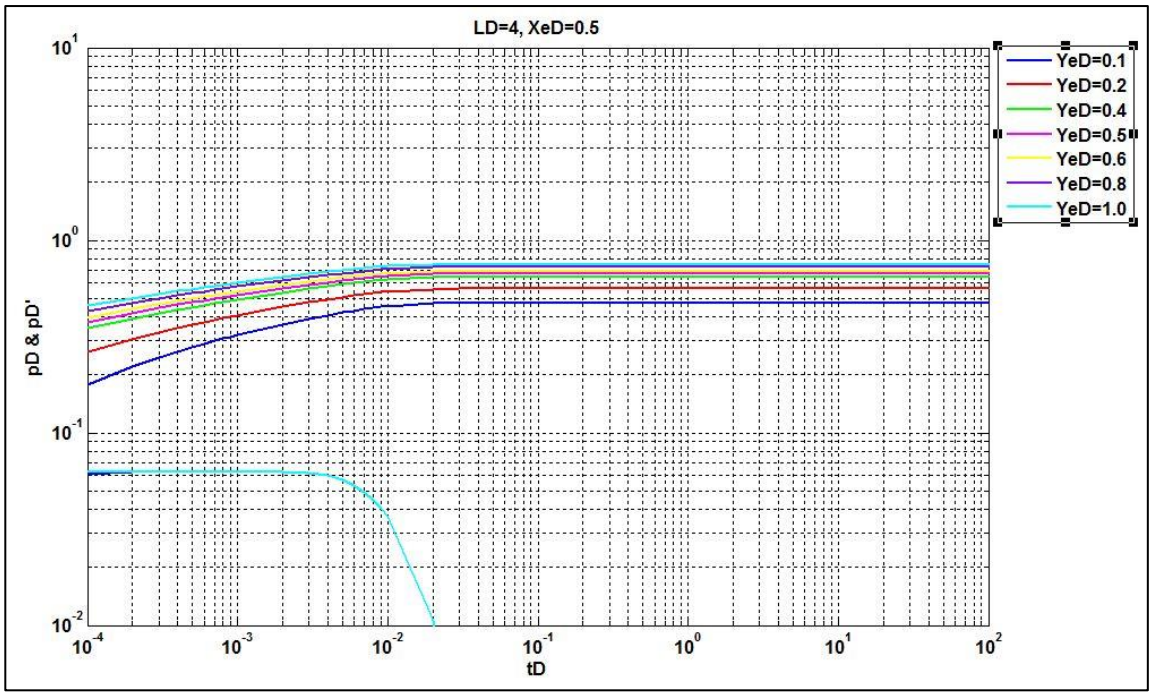

Figure 23: Type curve for short horizontal well, LD=4, XeD=0.5

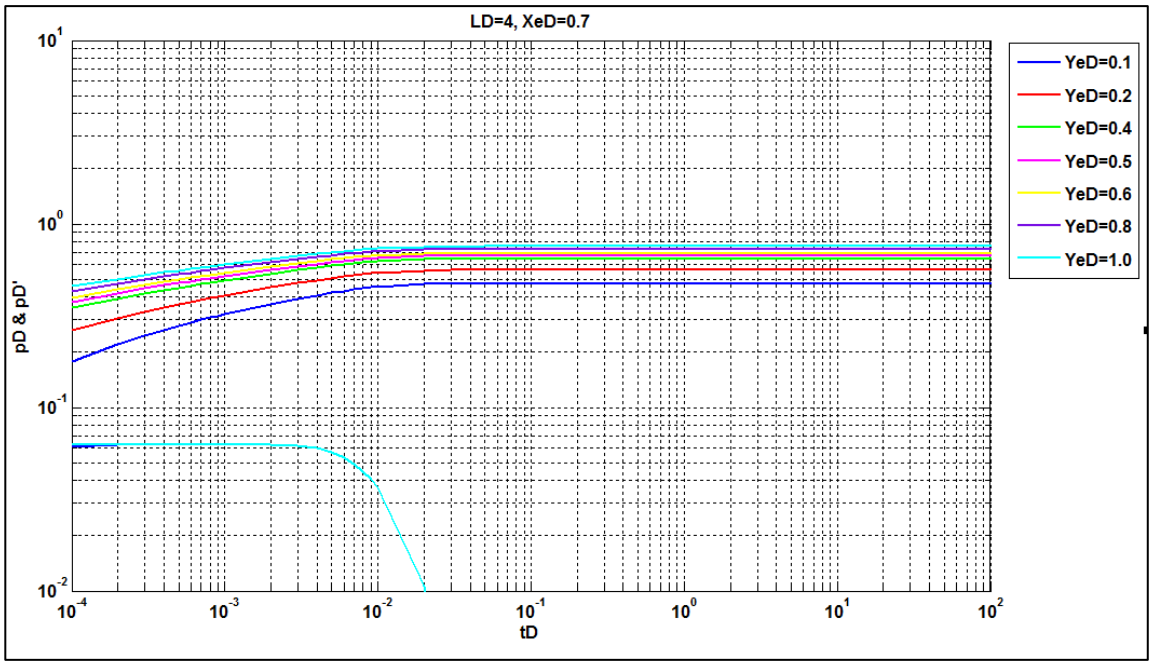

Figure 24: Type curve for short horizontal well, LD=4, XeD=0.7

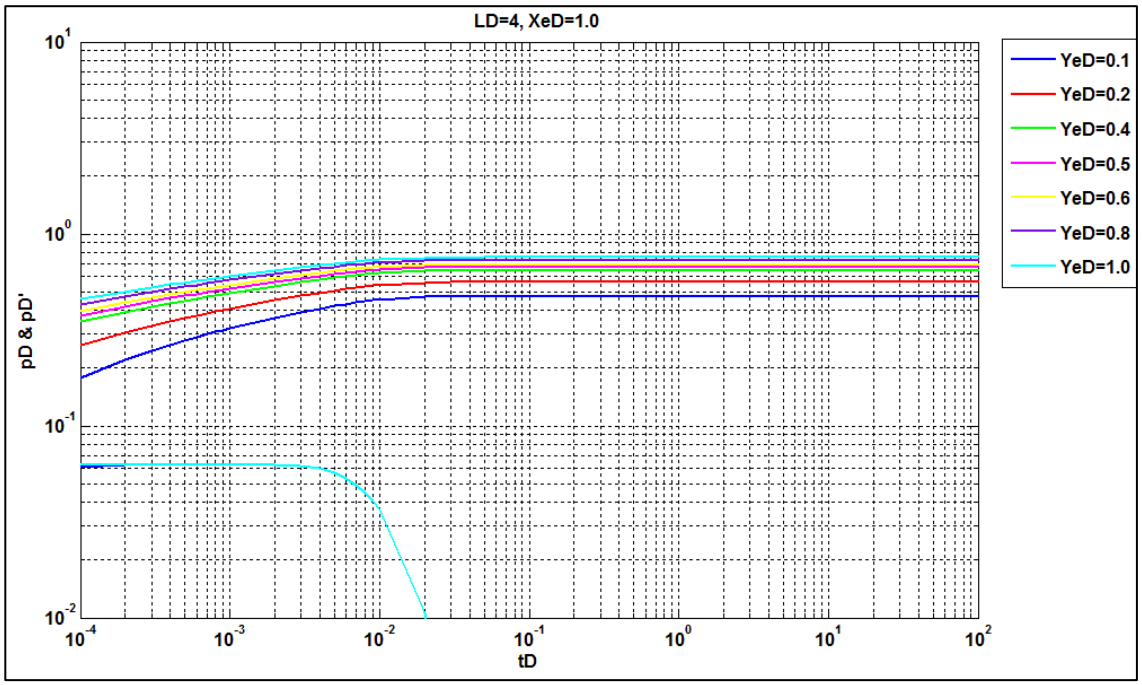

Figure 25: Type curve for short horizontal well, LD=4, XeD=1.0

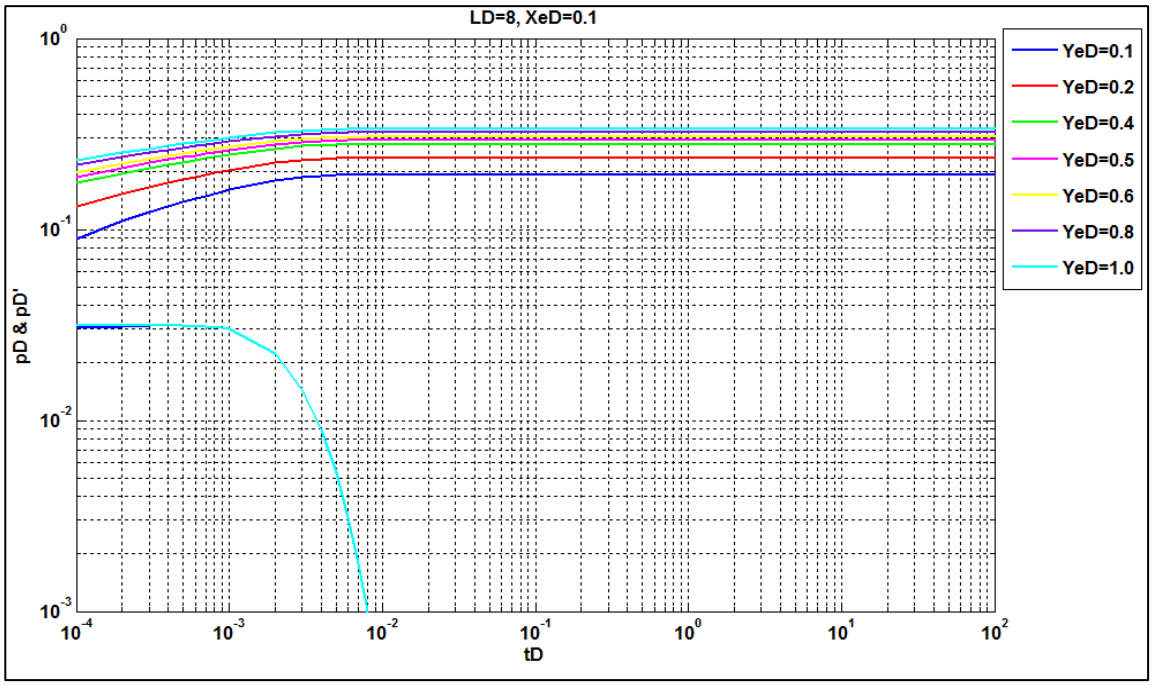

Figure 26: Type curve for short horizontal well, LD=8, XeD=0.1

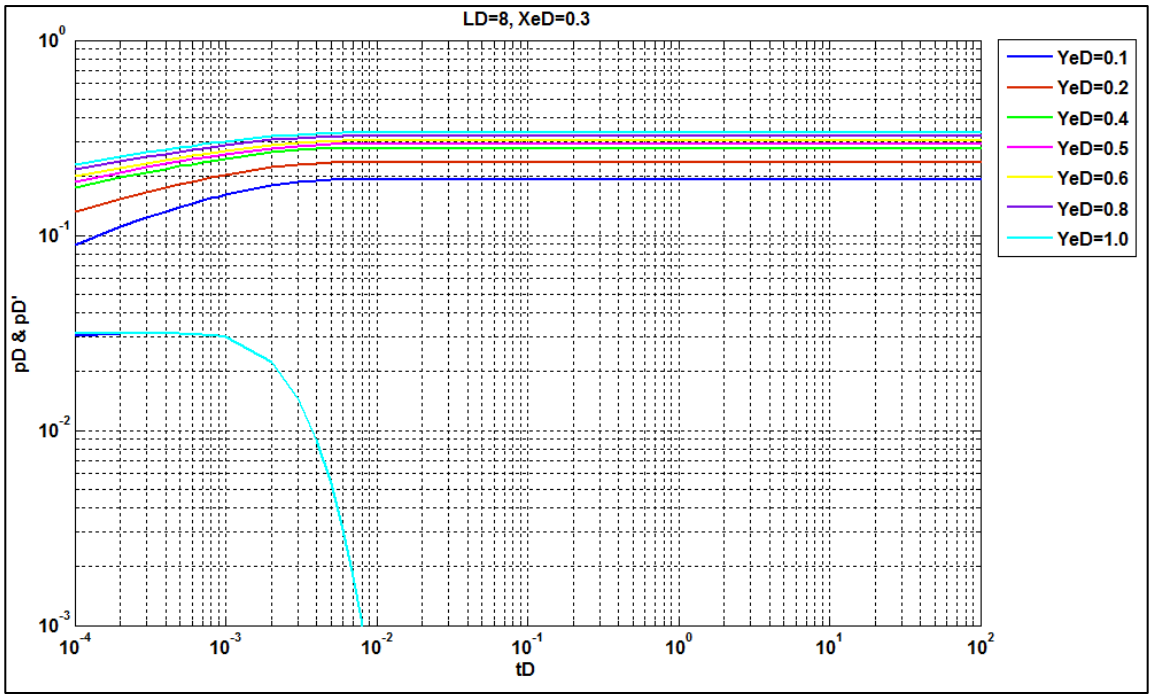

Figure 27: Type curve for short horizontal well, LD=8, XeD=0.3

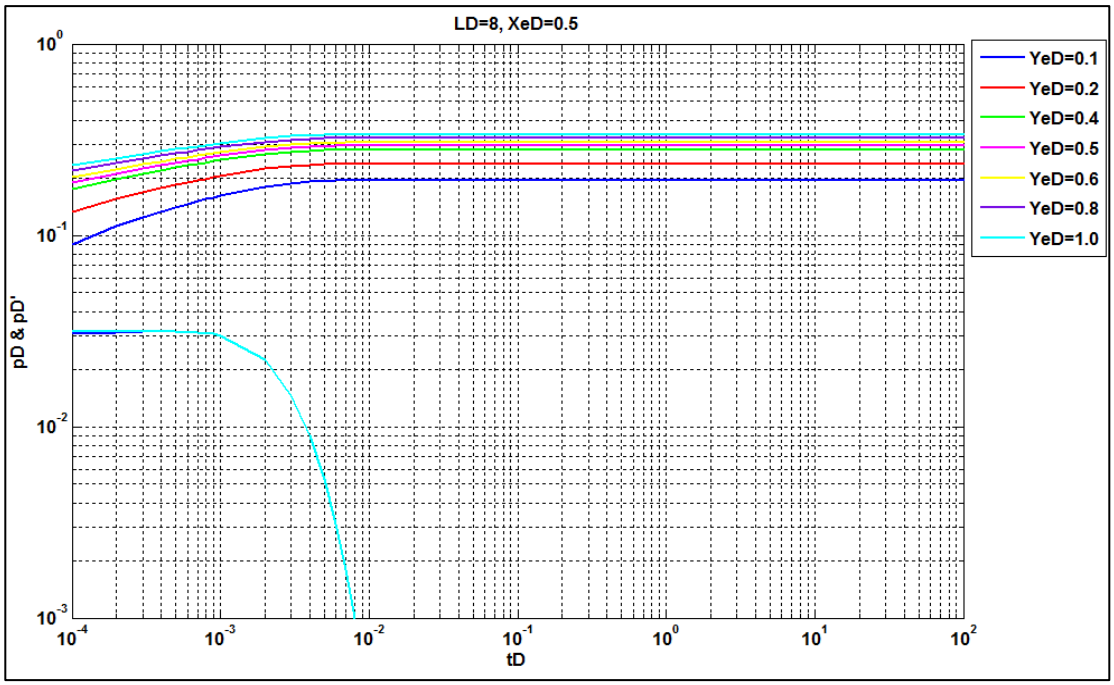

Figure 28: Type curve for short horizontal well, LD=8, XeD=0.5

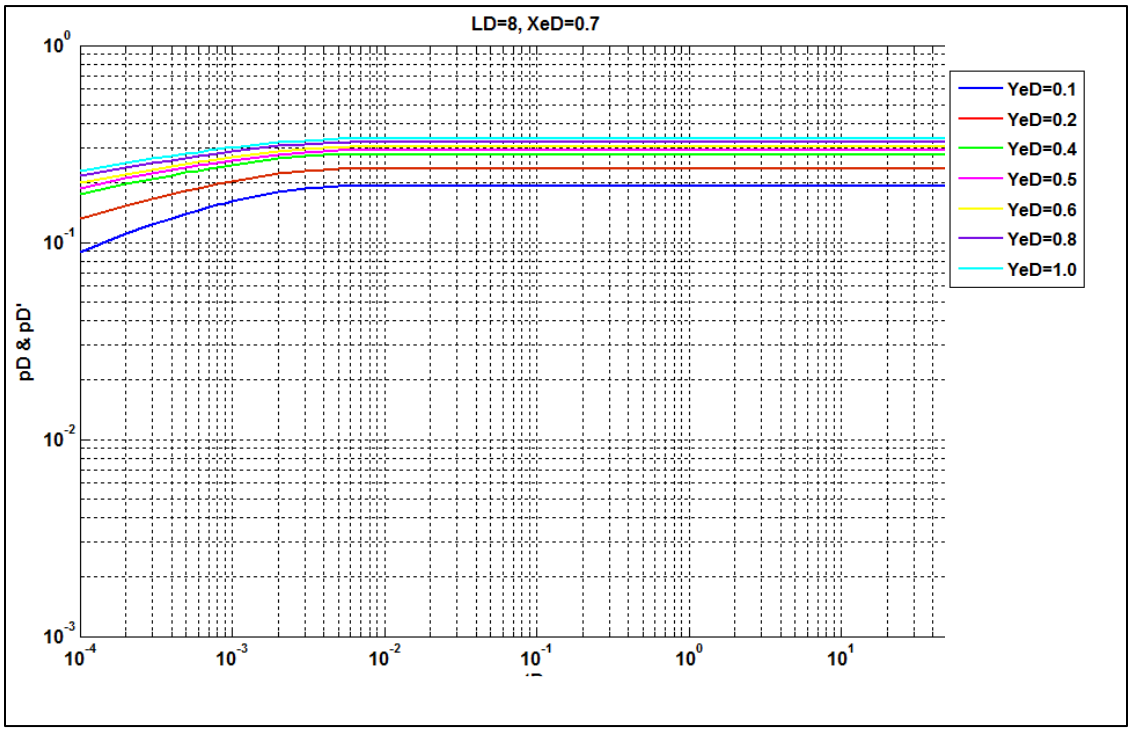

Figure 29: Short horizontal well, LD=8, XeD=0.7

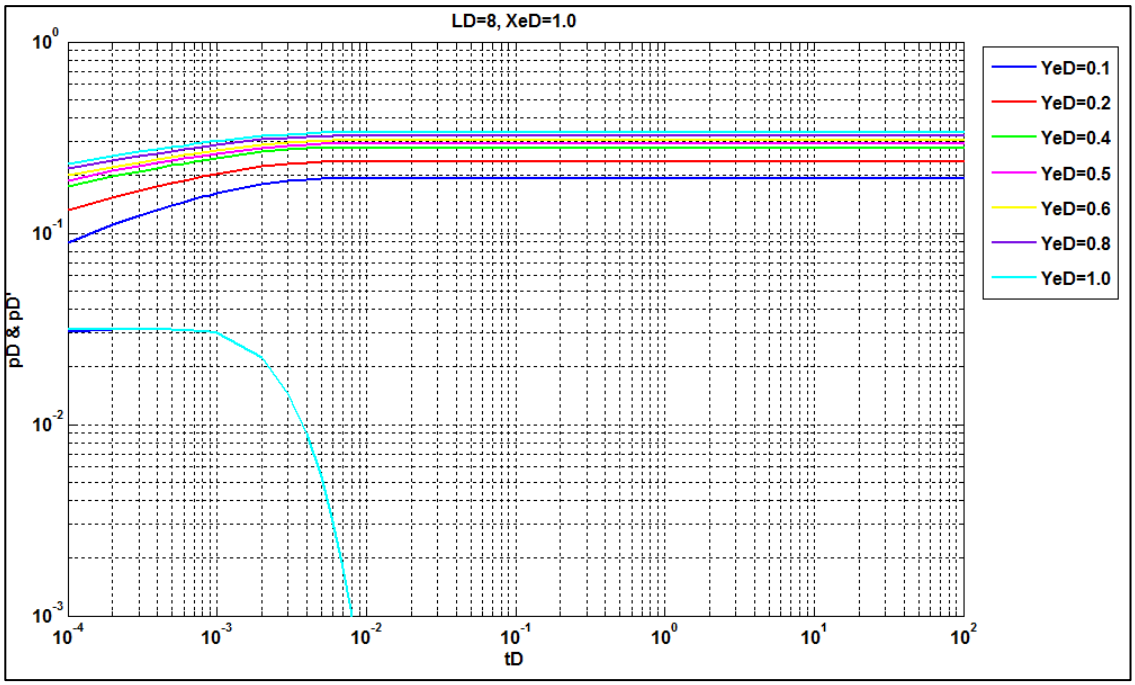

Figure 30: Type curve for short horizontal well, LD=8, XeD=1.0